Introducing Autonomous Vehicles: Adoption Patterns and Impacts on Social Welfare

Opher Baron[a], Oded Berman[a], Mehdi Nourinejad*[b]

[a]*Rotman School of Management, University of Toronto, Toronto, Canada*
[b]*Department of Civil Engineering, York University, Toronto, Canada*

Abstract

Problem definition: Autonomous vehicles (AVs) are predicted to enter the consumer market in less than a decade. There is currently no consensus on whether their presence will have a positive impact on users and society. The skeptics of automation foresee increased congestion, whereas the advocates envision smoother traffic with shorter travel times. We study the automation controversy and advise policymakers on how and when to promote AVs.

Academic / Practical Relevance: The AV technology is advancing rapidly and there is a need to study its impact on social welfare and the likelihood of its adoption by the public.

Methodology: We use supply-demand theory to find the equilibrium number of trips for autonomous and regular households. We develop a simulation model of peer-to-peer AV sharing. We compare the socially optimal level of automation with the selfish adoption patterns where households independently choose their vehicle type.

Results: We establish that the optimal social welfare is influenced by: (i) the network connectivity that is the ability of the infrastructure to serve AVs, (ii) the additional comfort provided by AVs that allows passengers to engage in other productive activities instead of driving, and (iii) the AV sharing patterns that reduce ownership costs, but create empty vehicle trips that increase congestion.

Managerial implications: We investigate the impact of AVs in a case study of Toronto and show that partial automation maximizes social welfare. We show that the comfort of AVs may add traffic that compromises social welfare. Moreover, although traffic increases with automation, travel times may decrease because of significant improvements in traffic flow caused by AV connectivity in the network.

1. Introduction

Autonomous vehicles (AV) are expected to radically change mobility patterns and improve the efficiency of transportation systems. The highest level of automation that is currently being tested on roads allows for vehicles to travel without a human on board. This concept opens abundant

opportunities as it increases road capacity, and introduces new ways of sharing vehicles among users. Because of these inherent benefits, more than 55 cities have committed to deploy AVs in the near future, and another 27 cities are preparing for automation by undertaking surveys of regulatory, planning, and governance issues raised by AVs (Bloomberg, 2017). The private sector is also actively pursuing vehicle automation. Almost all car manufacturers have currently established an AV division and expect to make the technology available to the mass market as early as 2025. By the year 2045, the AV market share is predicted to be as high as 87.2% (Bansal and Kockelman, 2017).

Upon their release to the public, AVs will promote collaborative consumption where vehicles are shared among multiple riders (Economist, 2016). To serve consecutive ride requests, the vehicles are relocated in driverless mode after dropping off one passenger to pick up the next one. Many car manufacturers have already recognized the emerging shareability of AVs and are planning to initiate their own ride-sharing programs. Ford recently released a plan to roll out Level-4 AVs designed for commercial ride-sharing applications by 2025 (Ford Media, 2017). General Motors is also developing automated Chevy Bolts for shared use, and Waymo (belonging to Google) is partnering with Chrysler to create a shared AV enterprise (City Lab, 2017).

One of the drawbacks of AV sharing is the induced traffic generated from relocation trips. These trips are known as zombie trips because they have zero occupants on board (Muoio, 2017). In addition to zombie trips, regular trips may also increase because the passengers experience additional comfort from engaging in alternative activities instead of driving. Many skeptics of automation claim that AV trips (both regular and zombie) will worsen traffic conditions and clog major urban streets. Some even argue that the average vehicle occupancy can get as low as 50% because of zombie trips and traffic may increase by up to 15% (Vox, 2017). In response to the skeptics, the advocates of automation believe AVs will make traffic smoother by reducing abrupt acceleration and braking, improving communications through vehicle-to-vehicle and vehicle-to-infrastructure channels, and reducing accidents. Several studies support promoting AVs. For instance, Atiyeh (2012) estimates that automation can increase speeds by 23-39% under fuel economy conditions and 8-13% in congested traffic. Reductions in accidents also improve traffic as 25% of congestion is attributed to traffic incidents in the U.S. (Fagnant and Kockelman, 2015). Moreover, paradigm improvements can appear in intersection control (traffic light design) when AVs reach high market-shares; a futuristic scenario is to have no traffic lights where cars clear the intersection in a synchronized manner without having to stop (Zhu and Ukkusuri, 2015).

AVs create new consumption patterns and business models. Toyota plans to transform from a car company into a mobility company that provides taxi service, while Ford envisions smart cities integrated with AVs. There are also new opportunities in software development that advance artificial intelligence, and new hardware technology that is more affordable, accurate, secure

and reliable. Among the new business models, peer-to-peer sharing allows a group of users to share a fleet of AVs with little to no profit-generating third-party interference. The *Decentralized Autonomous Vehicle* organization provides a Blockchain equipped platform where users offer and accept AV-related services (e.g., ride-sharing). In this peer-to-peer sharing company, AV owners and ride-seekers communicate directly using Blockchain, with no middleman taking part of the revenue (Forbes, 2018). Benjaafar et al. (2018) develops a strategic model of peer-to-peer sharing where consumers reduce their ownership costs by renting their purchased products (e.g., AVs) to other users that decide to rent in the market. Allahviranloo and Chow (2019) propose a "car club" where users gain fractional access to a fleet of AVs, similar to the timeshare model of owning real estate. In the private sector, General Motors plans to launch a peer-to-peer rental program, allowing GM vehicle owners to list their AVs to rent through the automaker's car-sharing platform, thus generating revenue for the company's vehicle owners (Washington Post, 2018).

In this paper, we address the controversy between the skeptics and advocates of vehicle automation by investigating the impacts of AVs on social welfare. The ridership model we consider is a peer-to-peer sharing service where a coalition of households has access to a fleet of AVs. We attempt to find if the increased network capacity from automation can serve the extra traffic generated from AVs. Our analysis and the insights it generates may support government agencies and other regulatory bodies in their study of the impacts of AVs.

Only a few studies focus on vehicle automation from an *operations management* perspective. Among them, Chen et al. (2017b) propose automated zones comprised of a set of streets allocated to AVs, Chen et al. (2016a) consider policies for managing a fleet of shared AVs, and Nourinejad (2018) studies the implications of parking provision in the era of AVs. While these policy-based studies are practically important, they are relevant when a reasonable fraction of a city's population has converted to AVs. There is still a lack of investigation on factors that promote travelers to switch to driverless modes while considering the benefits of drawbacks of automation.

Our main contribution is the study of the trade-off between induced traffic and infrastructure efficiency attained from automation. We show that three possible cases can occur in different cities. The cases recommend full, null, and partial automation. The cases are influenced by: (i) the network connectivity that is the ability of the infrastructure to serve AVs, (ii) the additional comfort provided by AVs that allows passengers to engage in other productive activities instead of driving, and (iii) the peer-to-peer sharing contract among users that reduces ownership costs but decreases the average vehicle occupancy (thus creating additional traffic).

Our methodology is based on supply-demand analysis, which is a fundamental concept in transportation economics (Ortuzar and Willumsen, 2002). We characterize the impact of automation on the equilibrium trips of AVs and regular vehicles and derive several insights. We show that AV owners travel more than regular vehicle owners because they can engage in alternative activities

while in the vehicle. Furthermore, although traffic increases with automation, travel times may decrease due to the positive impact of AVs on network capacity. In the case of no automation, the capacity improvement is not sufficient and AVs increase travel times. The benefits of AVs do not guarantee their adoption by the public, especially when households selfishly choose their vehicle type. We compare this user-based adoption pattern with the socially optimal level of automation, and recommend strategies that improve social welfare. The results show that AV sharing may not always reduce its usage cost enough to make it comparable to the price of regular vehicles. Thus, government intervention is required when there is a large price gap between both vehicle types.

We present a case study of the City of Toronto to validate our analytical findings and to present additional insights that were not possible to derive from the analytical model. We use actual traffic data to develop a simulation model that captures peer to peering sharing properties of AVs. Our model shows that partial automation maximizes social welfare in the downtown core of the City of Toronto.

The remainder of this paper is organized as follows. In Section 2, we review the related literature on vehicle automation. In Section 3, we present a supply-demand model for a mix of regular vehicles and AVs. In Section 4, we derive insights from the model and discuss the controversy between the skeptics and advocates of automation. In Section 5, we consider groups of heterogeneous users. In Section 6, we present a case study of peer to peer sharing. In Section 7, we provide conclusions. All proofs are in Appendix A.

2. Literature review

We look at the current state-of-practice in the auto industry and then discuss the literature on the capacity effects of automation, and vehicle sharing behavior. With recent advancements in automation technology, many provincial and state governments in North America, Europe, and South Asia are issuing permits for AVs to drive on designated roadways (Vox, 2017). Google, among the key investors in automated transportation, has tested driverless vehicles over more than 2 million miles in cities including Mountain View (since 2009), Austin (since 2015), Metro Pheonix (since 2016), and Kirkland (since 2016) (Waymo, 2016). The United States is a leader in the testing stage partly due to the *National Highway Traffic Safety Administration* who issued a set of national guidelines outlining the principles of driverless vehicle pilots (National Highway Traffic Safety Administration, 2013). These guidelines streamline the testing phase and motivate companies to pilot their prototypes in real-life traffic conditions. Canada is also starting several pilots in the province of Ontario and Quebec by allowing firms such as Uber to run their driverless vehicles in real streets (Allen, 2017).

An eminent stage that comes after the testing phase is regulation. There are 17 states in the U.S. pursuing AV-enabling legislature by passing bills to regulate operations and licensing

(Bansal and Kockelman, 2017). Regulatory policies include changing *traffic rules* to accommodate AVs (e.g., altering traffic light design), *land use intervention*, starting new *ride-sharing* services, initiating *pilot zones* (where AVs can be tested), *taxi reform* (i.e., automating taxis), *transit automation* (e.g., automating buses). There are cities that are taking a holistic approach to implement multi-faceted policies that target several aspects of automation together. Austin, for example, is among the cities taking the lead in automation.

The advanced technology used in AVs includes light detection and ranging systems, sensors, software, and additional computing power. The detection hardware can cost more than USD 30,000 (up to USD 100,000 for military uses) (Shchetko, 2014), but they are expected to become more affordable as AVs become available to the public on a mass scale. Hensley (2009) estimates that 15 years after the commercialization of AVs, their cost can drop from a USD 10,000 markup to a USD 3,000 markup. Before reaching these affordable markups, however, governing agencies may be able to promote AV purchases. Previous studies on electric vehicles highlight the impact of government intervention (Avci et al., 2014; Cohen et al., 2015; Raz and Ovchinnikov, 2015). We extend these studies by developing a framework that informs government agencies about the factors that influence the adoption of AVs by the public.

As AVs are considered an inevitable reality, a number of studies have investigated their impact in terms of fuel economy (Mersky and Samaras, 2016), induced traffic (Harper et al., 2016), willingness-to-pay for AVs (Bansal and Kockelman, 2017), traffic flow (Mahmassani, 2016; de Oliveira, 2017), intersection control (Yang and Monterola, 2016), AV parking (Nourinejad and Roorda, 2018), and the use of AVs as a shared fleet between a group of users

Two studies, Chen et al. (2017a) and Seo and Asakura (2017), show that network capacity generally increases with the AV market share due to platoon formation and lower reaction time of AVs. Both studies define a non-linear function that relates capacity to the share of AVs in the network. The highest capacity is reached when the entire traffic is automated. We use a similar capacity function. Our model also captures the zombie trip traffic flow resulting from AV sharing.

Emerging business models inspired by collaborative consumption have ushered in a new generation of transportation services (e.g., ride-sharing, car-sharing, and bike-sharing services) whereby travelers give up vehicle ownership for more flexible and affordable mobility. These transportation services are part of the sharing economy (Benjaafar and Hu, 2019; Hu, 2019). A significant body of literature is dedicated to vehicle-sharing services in the last decade that focuses on topics such as vehicle electrification (He et al., 2017), business models (Bellos et al., 2017), and peer-to-peer sharing (Tian and Jiang, 2017).

In addition to existing vehicle-sharing programs, another upcoming mobility pattern is to have a coalition of households share a fleet of AVs together without any involvement from profit-generating third parties. These coalitions allow households to divide the ownership cost of an

autonomous fleet between several entities to make it affordable. The AVs can self-relocate between multiple ride requests through the course of a day, thus serving multiple households. We present a simulation model of the City of Toronto and investigate the impacts of AVs with or without such coalitions on the social welfare.

3. Model

3.1. Households

Consider a region with N households; N_a households own an AV and $N_r = N - N_a$ households own a regular vehicle. For simplicity, we normalize the total number of households to $N = 1$.

Each regular household makes x_r trips per planning period (e.g., a day or a week), hence, the total regular vehicle volume is

$$v_r = N_r x_r. \tag{1}$$

The AV households make x_a trips [per planning period] and can share the vehicle with each other. Sharing a vehicle is possible because the AVs can self-relocate between multiple user requests. The relocation process, however, leads to zombie trips. To account for these trips, we assume that the relocation load in the network is l per trip. Hence, the total AV traffic volume is

$$v_a = N_a x_a (1 + l). \tag{2}$$

Assumption 1: The relocation load, l, is fixed and known.

According to Assumption 1, we keep the relocation load, l, as an exogenous parameter and assess its impact within its domain. In Section 6, we allow the relocation load, l, to be affected by the AV fleet size and demand characteristics. We show that the resulting relocation load is robust to these parameters.

3.2. The transportation network

Consider a transportation network with capacity c [trips per planning period]. AVs can improve traffic by using vehicle-to-vehicle technology and by communicating with traffic lights using vehicle-to-infrastructure technology (Chen et al., 2017a). Hence, when there are more AVs, the capacity of the network increases (Chen et al., 2017a; Seo and Asakura, 2017).

Let c_r and c_a be the network capacity when the entire traffic is exclusively made of regular vehicles or AVs, respectively. We assume $c_a \geq c_r$ because the network capacity is larger when the entire traffic is made of AVs. For a mixed traffic, the network capacity, c, depends on the ratio of the AV trip volume to the total volume:

$$r = \frac{v_a}{v_a + v_r}. \tag{3}$$

The function $c = C(r)$ is defined such that $C(0) = c_r$ and $C(1) = c_a$. For convenience and analytical tractability we assume:

Assumption 2: Network capacity $c = C(r)$ increases linearly with the AV ratio r such that

$$C(r) = c_r + r(c_a - c_r). \tag{4}$$

Using the capacity function from (4), we quantify the expected network travel time using a *Bureau of Public Roads* (BPR) type function (Chen et al., 2016b, 2017b) as:

$$T(v_a, v_r, c) = T_0 + \Big(\frac{v_a + v_r}{c}\Big)^b, \tag{5}$$

where T_0 is the free-flow travel time (the shortest travel in the network) and b is a parameter often equal to 3 or 4 (Button, 2010). Although T denotes a function, we also use T to refer to the value of the function when no confusions arise. Equation (5) is a slightly modified version of the standard BPR function that has all the same properties.

The opportunity cost of each hour of travel is β_r and β_a for regular and AV households, respectively. Intuitively, $\beta_r \geq \beta_a$ because AV passengers can engage in other activities such as texting (instead of driving). Hence, the travel cost of AVs and regular vehicles is $\beta_a\ T$ and $\beta_r\ T$ dollars per trip, respectively. We note that the AV households also incur a cost for vehicle relocation in occupant-free mode that is equal to qlx_a^*T where q is the cost of fuel and maintenance [dollars per hour]. This cost is small when q is insignificant especially when AVs are electrified. Moreover, in developed countries, ql is substantially smaller than the time-cost of AV owners β_a. Hence, we disregard the cost of vehicle relocation in the model.

3.3. Equilibrium of traffic volumes

Let $u(x)$ be the *marginal utility* [dollars per trip] for the x^{th} trip made at the household level with $\partial u(x)/\partial x < 0$ to represent diminishing returns (Huang et al., 2013). We assume all users are identical so that AVs and regular vehicles have the same *marginal utility* function $u(x)$.

Let x_a^* and x_r^* be the equilibrium trip volumes of AV and regular households, respectively. Then, $u(x)$ and $\beta_r T$ (or $\beta_a T$) form supply-demand type curves at the household level. Hence, the equilibrium volumes, x_r^* and x_a^*, are points where $u(x)$ intersects the travel cost functions:

$$u(x_i^*) = \beta_i T \qquad\qquad i = \{a, r\}. \tag{6}$$

3.4. Household utilities

We define U_a and U_r as the total utility obtained from trip-making by AV and regular households, respectively. These travel utilities are

$$U_i = \int_0^{x_i^*} u(x)\mathrm{d}x - \beta_i x_i^* T \qquad\qquad i = \{a, r\}. \tag{7}$$

The AV household utility may also include a hindrance term $h < 0$ that captures the reluctance of regular vehicle users to switch to AVs as in the adoption of any emerging technology. The hindrance may be psychological, such as the fear of traveling in a vehicle with no drivers, or technological and related to safety, security, and insurance. We may also impose a non-negative $h \geq 0$ illustrating the excitement of consumers for the automation technology. We assume $h = 0$ in the rest of the paper. As long as h is a constant, its impact on the qualitative results is limited.

Let f_r be the amortized ownership cost of a regular vehicle and f_a be the amortized cost of sharing an AV. We consider a peer-to-peer sharing model and discuss its properties in Section 6.

The net utility, B_i for $i = \{a, r\}$, captures the amortized ownership cost of a regular vehicle and the sharing cost of an AV:

$$B_i = \int_0^{x_i^*} u(x)\mathrm{d}x - \beta_i x_i^* T - f_i \qquad\qquad i = \{a, r\}. \tag{8}$$

We now define social welfare W as the weighted sum of the utilities:

$$W = U_a N_a + U_r N_r. \tag{9}$$

We note that social welfare does not include the ownership costs f_r and f_a as these expenses are internalized (they are revenues of car manufacturers who are valued beneficiaries of social welfare). The same argument is prevalent in the congestion pricing literature (Hassin and Haviv, 2003). The social welfare function may also include terms such as carbon emissions, accidents, and congestion. These terms are directly related to the level of traffic that is already captured in (9). Hence, with minor modification of certain parameters, (9) considers additional welfare aspects.

4. Social welfare and adoption patterns

In this section, we first derive the equilibrium number of trips in AV and regular households. We then derive the optimal level of automation desired by a social planner that maximizes the social welfare. Finally, we analyze selfish adoption patterns where each household decides its ideal mode (i.e., vehicle type).

4.1. Equilibrium conditions

In this section, we derive insights from the equilibrium conditions. Recall that AV households have a lower time-cost than regular households, i.e., $\beta_r \geq \beta_a$.

In the following lemma, we study the impact of β_r and β_a on the household trips x_r^* and x_a^*.

Lemma 1 (Offset in the number of trips)**.** *Let $u^{-1}(.)$ be the inverse of the marginal utility function. Then, we have*

$$x_r^* = u^{-1}\Big(u(x_a^*)[\beta_r/\beta_a]\Big). \tag{10}$$

When the marginal utility is the well-known power function $u(x) = x^{-1/\gamma}$, with $\gamma > 1$ capturing sensitivity to trips (Petruzzi and Dada, 1999; Ray et al., 2005), we have

$$x_a^* = x_r^*(\beta_r/\beta_a)^\gamma. \tag{11}$$

From here on, we use the power marginal utility function in our analysis, which allows us to derive a closed-form expression for performance measures. For the exponential function and other marginal utilities functions, we perform numerical experiments. The results of these experiments are reported in Section 4.2, where we show that they qualitatively agree with the closed form results derived below.

According to Lemma 1, AV households travel more than regular households because AV occupants can engage in other activities instead of driving.

We now explore the properties of the equilibrium under Assumptions 1 and 2. For the power demand function in (11), we write the ratio r of AVs to total volume from (3) using the definitions of v_a and v_r in (1-2) as

$$r = \frac{N_a(1+l)(\beta_r/\beta_a)^\gamma}{N_a(1+l)(\beta_r/\beta_a)^\gamma + N_r}. \tag{12}$$

Substituting r from (12) into the capacity function from (4), we get

$$C = \frac{c_a N_a(1+l)(\beta_r/\beta_a)^\gamma + c_r N_r}{N_a(1+l)(\beta_r/\beta_a)^\gamma + N_r}, \tag{13}$$

which is a convex combination of c_r and c_a where the weights are the number of regular households N_r, and AV households $N_a(1+l)(\beta_r/\beta_a)^\gamma$ adjusted by the relocation load l and the time-cost ratio β_r/β_a.

For the power demand function per (11), the travel time function from (5) becomes

$$T = T_0 + \Big(x_r^* \ \frac{N_a(1+l)(\beta_r/\beta_a)^\gamma + N_r}{C}\Big)^b, \tag{14}$$

which has the following interpretation. When $\beta_r = \beta_a$, the total traffic volume is $v = x_r^*[1 + lN_a]$, indicating that all households make x_r^* trips in addition to an extra l zombie trips made by the N_a AV households. Thus, AV households create more traffic than regular households because of the relocation load; this extra traffic harms social welfare because it is a dead-weight on the network. When the relocation load is $l = 0$, only the impact of AVs remains and the total traffic volume is $v = x_r^*\big(1+N_a[(\beta_r/\beta_a)^\gamma - 1]\ \big)$, i.e., all households make x_r^* trips in addition to an extra $(\beta_r/\beta_a)^\gamma - 1$ (where $\gamma > 1$) trips made by the N_a AV households because of their lower time-cost. Thus, AVs

households create more traffic than regular households but gain a higher utility because of the enhanced comfort of AVs.

We now define the *adjusted capacity*, $\bar{C}$, as:

$$\bar{C} = \frac{c_a N_a (1+l)(\beta_r/\beta_a)^\gamma + c_r N_r}{[N_a(1+l)(\beta_r/\beta_a)^\gamma + N_r]^2}, \tag{15}$$

which depends on N_a since c_i and β_i, where $i = \{a, r\}$, are parameters, and $N_r = 1 - N_a$.

With this definition, the travel time function from (14) becomes

$$T = T_0 + \left(\frac{x_r}{\bar{C}}\right)^b. \tag{16}$$

We note that (5) uses the total traffic volume to derive the travel time, whereas (16) derives travel time as a function of household trips. Thus, (16) transforms (5) from the network level to the household level.

According to (16), the travel time is a function of the *adjusted capacity* $\bar{C}$ and the number of trips x_r. Hence, we have $T = T(x_r, \bar{C})$. Alternatively, one may also rewrite (16) as a function of the AV household trips such that $T = T_0 + (x_a/\bar{C})^b$ where $\bar{C}$ has to be redefined.

4.2. Maximizing social welfare

In this section, we explore the impact of AV households on the utility. Given $T = T(x_r, \bar{C})$, we rewrite utility as

$$U_i = \int_0^{x_i^*} u(x)\mathrm{d}x - \beta x_i^* T(x_i^*, \bar{C}) \qquad\qquad i = \{a, r\}, \tag{17}$$

where $\bar{C}$ depends on N_a per (15). Consequently, social welfare W also depends only on N_a.

We next analyze the social welfare under the power-utility function. According to (7) and (11)

$$U_a = (\frac{\beta_r}{\beta_a})^{\gamma-1} U_r, \tag{18}$$

which simplifies the social welfare function to

$$W = U_a\big(N_a + (1-N_a)(\beta_r/\beta_a)^{\gamma-1}\big). \tag{19}$$

The time-costs, β_a and β_r, affect two parts of the model: (i) the equilibrium conditions (6), i.e., $u(x_i^*) = \beta_i T$, and (ii) the social welfare function $W = N_a U_a + N_r U_r$ in (9). We note that (19) already considers that the equilibrium conditions in (6) hold and the AV users travel more than regular vehicle owners according to Lemma 1. However, the social welfare, W, in (19) is difficult to analyze analytically. Thus, we approximate it by changing the cost ratio. Specifically, we substitute $(\frac{\beta_r}{\beta_a})^{\gamma-1} = 1$ into (19). This approximation assumes that the planner weighs time-

costs equally, i.e., independent of their mode choice. To summarize, based on (18) and (19) we approximate the social welfare as:

$$\hat{W} = U_a = (\frac{\beta_r}{\beta_a})^{\gamma-1} U_r. \tag{20}$$

The approximation error is $\epsilon = \frac{W-\hat{W}}{\hat{W}}$. Using (19) and (20), for any automation level, N_a, the approximation error is:

$$\epsilon = (1 - N_a)\Big(1 - (\beta_a/\beta_r)^{\gamma-1}\Big). \tag{21}$$

Note that as γ is typically close to 1 and β_r is close to β_a, the error approaches zero. At $N_a = 1$ the error is also zero. The error is bounded from above by $1 - (\beta_a/\beta_r)^{\gamma-1}$. As the fraction $(\beta_a/\beta_r)^{\gamma-1}$ is smaller than 1, the automation level that maximizes $\hat{W}$ provides a good approximation for the automation level that maximizes W.

In the following analysis we let $\tau = (\beta_r/\beta_a)^{\gamma}$ be the time-cost ratio. We also use $\hat{N}_a^*$ and N_a^* to denote the levels of automation that maximize the approximate social welfare, $\hat{W}$, and the actual social welfare, W, respectively. We note that the AV level, $\hat{N}_a^*$, that maximizes $\hat{W}$ simultaneously maximizes the utilities U_a and U_r, because of (18).

Proposition 1 (Optimal social welfare automation level approximation)**.** *The approximate social welfare, $\hat{W}$, is maximized at the AV level $\hat{N}_a^*$ given by:*

$$\hat{N}_a^* = \begin{cases} 1 & \dfrac{1}{2-\tau(1+l)} \le \dfrac{c_a}{c_r} \quad (22a) \\ \dfrac{c_r + \tau(1+l)(c_a - 2c_r)}{\big(\tau(1+l)-1\big)\big(c_a\tau(1+l) - c_r\big)} & \dfrac{2\tau(1+l)-1}{\tau(1+l)} \le \dfrac{c_a}{c_r} < \dfrac{1}{2-\tau(1+l)} \quad (22b) \\ 0 & \dfrac{2\tau(1+l)-1}{\tau(1+l)} > \dfrac{c_a}{c_r}\,. \quad (22c) \end{cases}$$

We now show the following insight on the true social welfare, W:

Proposition 2 (Impact of the time-cost ratio on the social welfare)**.** *The level of automation, N_a^*, that maximizes the true social welfare first decreases then increases with the time-cost ratio, $\tau \in [1, \infty)$.*

As an example of Proposition 2, Fig. 1 presents the optimal automation level, N_a^*, that maximizes the social welfare W. Fig. 1a presents N_a^* as a function of the time cost ratio τ. When $\tau = 1$, $\frac{\partial N_a^*}{\partial \tau} < 0$ because the AV users travel more and add traffic that ultimately decreases the social welfare; Thus, automation decreases the social welfare. In contrast, when τ is significantly bigger than 1, then $\frac{N_a^*}{\partial \tau} > 0$ because although AVs increase traffic, their users experience a low discomfort from traveling because of their small time-cost. Thus, automation increases social welfare. The proof of Proposition 2 establishes this behavior analytically.

In Fig. 1b, we vary the capacity ratio, c_a/c_r, and present the optimal AV level, N_a^*. The capacity ratio increases the optimal AV level due to higher connectivity in the network. Moreover, in both Fig. 1a-b, the optimal AV level, N_a^*, decreases with the relocation load, l, because of the additional congestion caused by zombie trips.

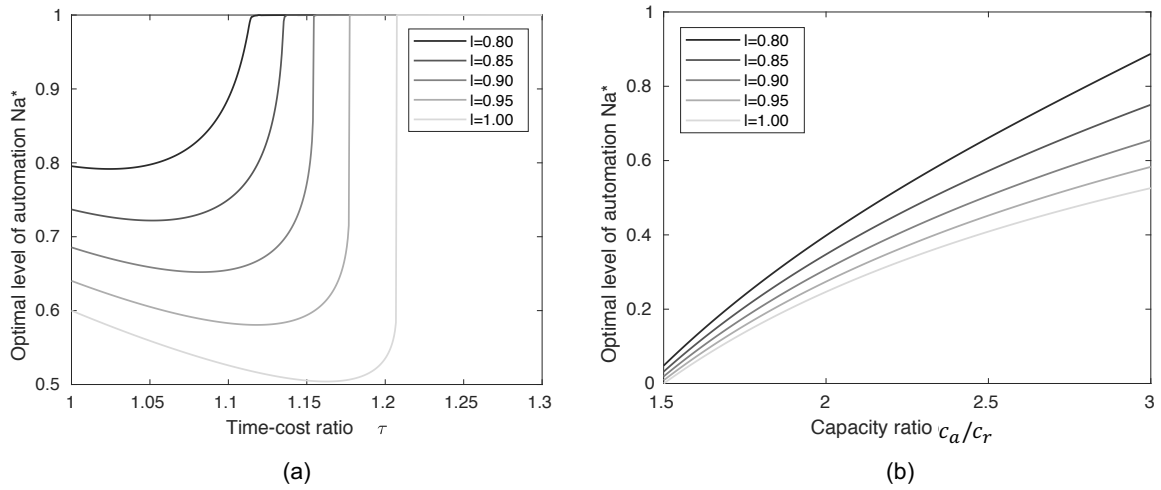

Figure 1: Optimal level of automation N_a^* at varying relocation loads, l with (a) varying time-cost ratios, τ, and (b) varying capacity ratios, c_a/c_r. The parameters are: $\gamma = 5, b = 4, T_0 = 0$.

We next consider two special cases where the entire traffic is made of either AVs or regular vehicles.

Proposition 3 (The extremes of automation)**.** *For a negligible free-flow travel time, $T_0 = 0$, the social welfare at full-automation is larger than (or equal to) the social welfare at no-automation if and only if $c_a/c_r \geq (1+l)(\beta_a/\beta_r)^{1/b}$.*

When $c_a/c_r \geq (1+l)(\beta_a/\beta_r)^{1/b}$, the all-AV case is better than the no-AV case, because AVs improve the network capacity, which leads to a larger x_r^* (and x_a^*) and a larger utility. In contrast, when $c_a/c_r < (1+l)(\beta_a/\beta_r)^{1/b}$, the all-AV case is worse than the no-AV case, because (i) AVs require a large relocation load l that reduces x_r^* (and x_a^*) and the utility, or (ii) the AV households have a low cost of time β_a and travel more than regular households.

As an example of Proposition 3, consider equal time costs, $\beta_a = \beta_r$, and a capacity ratio of $c_a/c_r = 1.4$ according to Chen et al. (2017b). Then, per Proposition 3, the social welfare is larger at full than no automation if $l < 0.4$.

The insight here is the presence of a trade-off in the number of AVs in the network. While AVs improve the network capacity as $c_a \geq c_r$, they add zombie trips to the network that compromise the network capacity. Moreover, AV users also travel more due to the lower time-cost and thus put a larger load on the network. Thus, sharing reduces social welfare because it leads to zombie trips that increase congestion. In contrast, automation may positively or negatively impact social welfare depending on the time-cost ratio β_a/β_r and the network capacity ratio c_a/c_r.

We now derive insights from Propositions 1 and 3. We show that according to the capacity ratio c_a/c_r, the extra load function $L(m,n)$, and the time-cost ratio β_r/β_a, there are three possible cases for the shape of social welfare, W, as shown in Fig. 2.

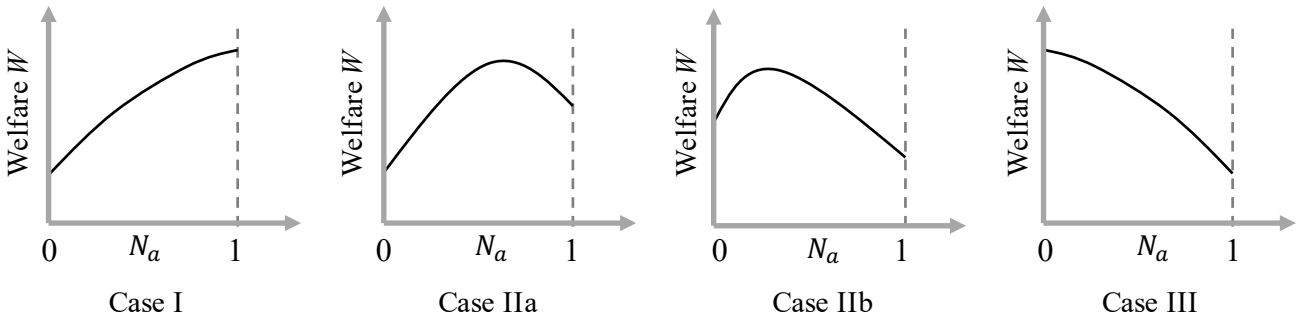

Figure 2: Three possible social welfare cases.

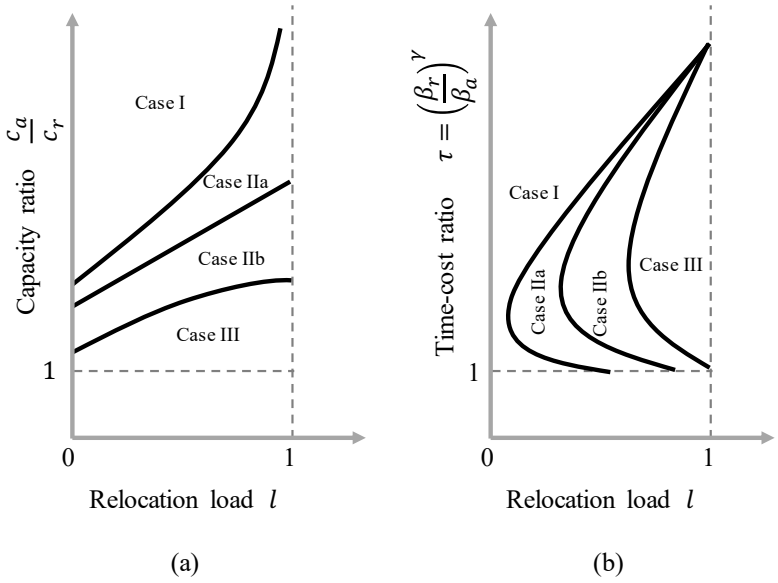

Figure 3: Three possible utility cases. The area $c_a/c_r < 1$ and $\tau < 1$ are infeasible. We do not show a plot of the capacity ratio against the time-cost ratio as it is schematically similar the panel (a).

Case I [Equation (22a)]: Social welfare strictly increases with the AV penetration N_a. Hence, it is ideal to have full-automation with $N_a = 1$, because the capacity ratio c_a/c_r is large enough to absorb the relocation load l. Moreover, the time-cost ratio $(\beta_r/\beta_a)^\gamma$ is small indicating that AVs are comfortable enough to induce additional traffic that compromises the capacity of the network.

Case IIa [Equation (22b)]: Social welfare is higher at $N_a = 1$ compared to $N_a = 0$. Moreover, the optimal $\hat{N}_a^*$ is between 0 and 1. Hence, partial automation leads to the optimal W.

Case IIb [Equation (22b)]: Social welfare is higher at $N_a = 0$ compared to $N_a = 1$. Moreover, the optimal $\hat{N}_a^*$ is between 0 and 1. Hence, partial automation leads to the optimal W. Occurrence of Case IIa and IIb is a result of a trade-off between the capacity, time-cost, and relocation load.

Case III [Equation (22c)]: Social welfare strictly decreases with N_a. Hence, it is ideal to have no-automation with $N_a = 0$, because the capacity ratio c_a/c_r is small and cannot absorb the relocation load. Moreover, the time-cost ratio $(\beta_r/\beta_a)^\gamma$ is large indicating that the extra comfort experienced by AV owners may induce traffic that compromises the capacity of the network.

In Fig. 3 we depict the boundaries of the three cases. The different regions inform policymakers about the extent of the benefit that can be achieved through optimal policies. For example, in Case I, any action to promote automation improves social welfare, whereas in Cases II, automation can reduce social welfare if imposed inadvertently, and in Case III, it is not wise to automate at all. In Fig. 3a, increasing the capacity ratio, c_a/c_r, always improves the optimal level of automation, N_a^*, and the social welfare. In Fig. 3b, increasing the time-cost ratio, τ, may first decrease then increase the optimal level of automation, N_a^*, per Proposition 2.

The three cases also demonstrate the controversy between the advocates and skeptics of vehicle automation. The advocates claim that AVs are beneficial for social welfare because they reduce traffic and improve social welfare whereas the skeptics argue that AVs cause significant zombie trips that lead to higher traffic and lower social welfare. We clarify this discussion by showing that the degree of AV penetration depends on the trade-off between network connectivity, represented by the capacity ratio c_a/c_r, the comfort from the time-cost ratio represented by β_r/β_a, and the peer-to-peer sharing contract among users (which reduces ownership costs but leads to zombie trips) represented by l (ownership costs are discussed in the next section). Hence, any rational judgment of AV impacts rests on one of the cases; depending on the conditions outlined by the cases, either the advocates or the skeptics may be correct.

We present a supplementary interpretation of the three factors. The capacity ratio c_a/c_r is related to the ability of infrastructure to serve AVs. For example, Audi, is connected to more than 2,250 traffic lights of ten cities in the U.S. including Phoenix, and Washington D.C (Audi, 2016); vehicle-to-infrastructure (V2I) connectivity enables the Green-Light-Optimized-Speed-Advisory system, which recommends the optimal cruising speed in order to sail through each open signal, thus maximizing the throughput at intersections. Naturally, cities equipped with V2I technology have a higher capacity ratio c_a/c_r and are more competent hosts of AVs due to their infrastructure.

The peer-to-peer sharing contract and the relocation load $l = L(m, n)$ are influenced by the sharing tendencies of each city's residents. Cities such as Seattle, Vancouver, and Washington D.C. demonstrate the propensity to share vehicles; in Washington D.C. each carsharing vehicle replaces about 3-8 personally owned vehicles (Martin and Shaheen, 2016). Among these cities, Vancouver has the highest population density (of 54,000 persons per km^2), which creates better sharing opportunities and consequently a lower relocation load l.

The final influencing component is the AV itself and the level of comfort it provides, which directly impacts the time-cost ratio β_r/β_a. Volvo is currently designing a concept car (Volvo 360)

that offers passengers an on board bed, similar to but more comfortable than reclining aircraft seats. The time-cost ratio β_r/β_a for this vehicle is large because the passengers experience little discomfort from traveling. Thus, the additional traffic from the Volvo 360 may compromise social welfare unless the AV time-cost, β_a is very small because of the high comfort of this vehicle. In contrast, the smart vision EQ for-two is a Mercedes initiative that is not as comfortable as the Volvo 360. Thus, this vehicle has a smaller ratio β_r/β_a (at least smaller than the time-cost ratio of the Volvo 360), and may increase traffic and reduce social welfare.

There is an alternative way of interpreting the policy space in Fig. 3 that focuses on the long-term effects of AVs. Cities are not stagnant and change constantly with enhanced infrastructure. Thus, the no-automation recommendation of Case III may change as infrastructure improves and the capacity ratio c_a/c_r increases; Case III may become Case II and finally Case I over time. Hence, the recommendations of the policy space is temporary but gives perspective on the path required to reach a desirable levels of automation. In a similar way, the time-cost ratio and the relocation load are also subject to changes as newer versions of AVs provide increasing comfort and as emerging business models allow for more effective sharing.

The following proposition discusses the special conditions of the three cases.

Proposition 4 (Special scenarios)**.** *Consider the following four scenarios under approximate social welfare maximization:*

1. *When the capacity ratio is large such that $c_a/c_r \geq 2$, then some level of automation is always beneficial. This eliminates Case III.*

2. *Suppose the time-costs are equal $\beta_a = \beta_r$, and the relocation load is large $l = 1$. Then, full automation is never beneficial, i.e., Case I does not occur.*

3. *Suppose again $\beta_a = \beta_r$ and $l = 0$. Then, full automation is recommended. This condition exclusively leads to Case I, which occurs when the AV households choose to own their personal vehicles instead of sharing.*

4. *When $(\beta_r/\beta_a) > 2^{1/\gamma}$, full automation is not recommended. This eliminates Case I, which occurs when the time-cost of AV households is smaller than regular households.*

Proposition 4 gives rules-of-thumb on the impact of automation under special conditions. The four scenarios require little knowledge of the travel time or the marginal utility function parameters. According to Scenario 1, automation is beneficial if AVs can at least double the network capacity; in Scenarios 2 and 3, recommendation of full automation depends on the relocation load l; and in Scenario 4, full-automation depends on the time-cost ratio.

4.3. Mode choice equilibrium

We have so far considered automation levels that maximize social welfare, ignoring the vehicle ownership costs. Socially optimal solutions are not always preferred if the users are able to switch

to another mode and receive a higher net utility. When the ownership costs are included, users may have a preference toward one of the vehicle types, e.g., an expensive AV may not be preferred regardless of its positive impact on traffic flow.

The *net utilities* in (8) dictate the user mode choices as follows. An equilibrium is reached under Wardrop's law (Wardrop, 1952) if (i) no household can change its vehicle type and increase its net utility, and (ii) each household maximizes its net utility.

We use N_a° and $N_r^\circ = 1 - N_a^\circ$ to denote the mode choice equilibrium shares of autonomous and regular households, respectively. According to Wardrop's two conditions, the mode choice equilibrium is defined as the following.

Proposition 5. *[Wardrop's principles in mathematical terms] If the net utilities are unequal, $B_a(N_a) \neq B_r(N_a), \forall N_a \in (0,1)$, then we have an all-or-nothing assignment where $N_a^\circ = 1$ if $B_a(N_a = 1) > B_r(N_a = 0)$ and $N_a^\circ = 0$ if $B_a(N_a = 1) < B_r(N_a = 0)$. In contrast, if $B_a(N_a^\circ) = B_r(N_a^\circ)$ for some $N_a^\circ \in (0,1)$, an intermediate equilibrium $N_a^\circ \in (0,1)$, may occur. The intermediate equilibrium is unstable if*

$$\frac{\mathrm{d}B_a(N_a^\circ)}{\mathrm{d}N_a} > \frac{\mathrm{d}B_r(N_a^\circ)}{\mathrm{d}N_a}. \tag{23}$$

Moreover, an equilibrium solution always exists and is unique.

According to (23), the equilibrium is unstable if minor perturbations in the automation level, N_a°, decrease the net utility of households with either of the two choices. For example, if we increase the automation level N_a by $\mathrm{d}N_a$, the AV households receive a higher net utility than regular households. Here, regular households perceive this change as beneficial and convert. Thus, the original equilibrium is unstable.

We next investigate the mode choice equilibrium for each case. For Case I, Fig. 4 presents all possible mode choice equilibria. In Fig. 4a, the net utilities of AV and regular households do not intersect. Hence, we have an all-or-nothing solution. Because $B_a(N_a = 1) > B_r(N_a = 0)$, we have $N_a^\circ = 1$. In contrast, in Fig. 4b is also an all-or-nothing but $N_a^\circ = 0$ because $B_a(N_a = 1) < B_r(N_a = 0)$. In Fig. 4c, both net utilities intersect, however, the resulting equilibrium is unstable because regular households can change their mode and receive a higher net utility. Thus, a single equilibrium point occurs at $N_a^\circ = 1$. Fig. 4d is also all-or-nothing where $N_a^\circ = 1$ because B_a is strictly larger than B_r. Thus, all possible equilibria in Case I are all-or-nothing.

For Case I, we compare the mode choice equilibrium N_a° with the socially optimal level of automation $\hat{N}_a^* = 1$ from (22a). According to Fig. 4, the mode choice equilibrium and the socially optimal $\hat{N}_a^*$ are equivalent except for Fig. 4b where the AV ownership cost is high. Governing agencies can eliminate such adverse situations by promoting suitable policies. For instance, subsidization of AVs improves affordability and ultimately increases social welfare; the minimum subsidy to eliminate the occurrence of Fig. 4b is $B_r(N_a = 0) - B_a(N_a = 1)$.

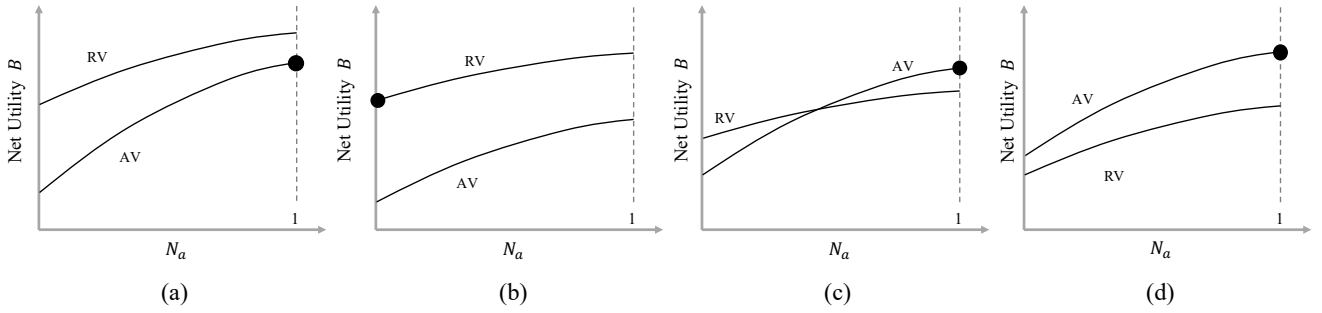

Figure 4: The net utility of AV and regular vehicle (RV) households in Case I. The circle is the mode choice equilibrium point.

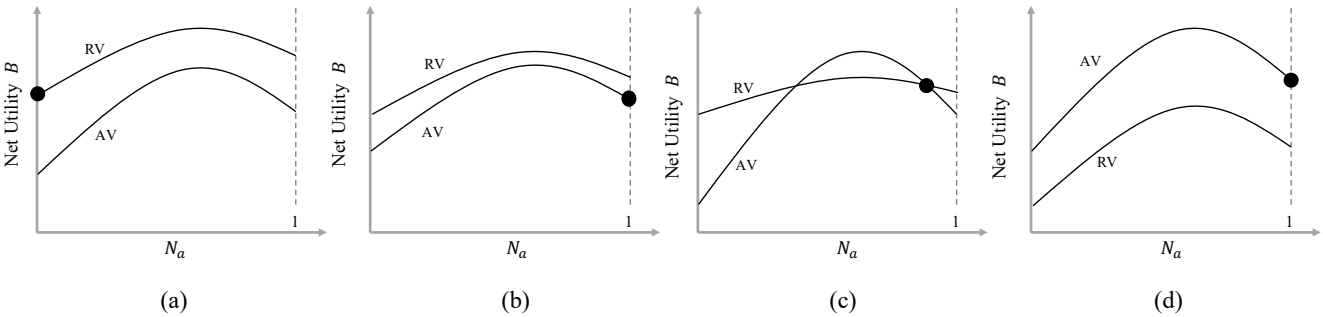

Figure 5: The net utility of AV and regular vehicle (RV) households in Case II. The circle is the mode choice equilibrium point.

For Case II, Fig. 5 presents the mode choice equilibria for Case IIa. We have all-or-nothing equilibrium except in Fig. 5c where two intermediate intersections occur in $N_a \in (0, 1)$. From the two points, only one is stable. Similar figures, with similar findings, for case IIb are omitted.

For Case III (figures are omitted), according to Proposition 1, $\hat{N}_a^* = 0$. The mode choice equilibrium and the socially optimal $\hat{N}_a^* = 0$ are typically equivalent. Governing agencies can eliminate such adverse situations using suitable policies. For instance, in such cases, taxation of AVs increases social welfare and reduces network travel time.

5. Heterogeneous travelers

We now extend the model to consider heterogeneous travelers. We first derive the automation level that maximizes social welfare. Then, we look at the mode choice equilibrium. We consider a special case of heterogeneity, and discuss the more general setting in Appendix B.

5.1. Maximizing social welfare with heterogeneous travelers

Consider a Set J of heterogeneous groups of users where group $j \in J$ has a population of p^j households that experience a marginal travel cost of β_r^j and β_a^j for owning a regular or autonomous vehicle, respectively, such that $\beta_r^j \geq \beta_a^j, \forall j \in J$. We assume that the time-costs ratio is constant among all groups such that $\beta_r^j/\beta_a^j = (\tau)^{1/\gamma}$ where $\tau \geq 1$ and $\gamma > 1$ (for the power utility function)

are parameters. We assume that the relocation load is identical among the groups, i.e., $l^j = l, \forall j \in J$. We perform numerical experiments to assess the impact of these two assumptions (results are reported at the end of this section).

The proportion of group j AV and regular households is N_a^j and N_r^j, respectively, where $N_r^j = 1 - N_a^j, j \in J$. Each household of group j and type $i = \{a, r\}$ makes x_i^j trips; let $X = \{x_i^j\}$ be the vector of household trips.

The AV and regular vehicle traffic volume are given respectively by

$$v_a = \sum_j p^j N_a^j x_a^j (1 + l) \qquad \text{and} \qquad v_r = \sum_j p^j N_r^j x_r^j. \tag{24}$$

The total traffic volume is $v = v_a + v_r$ and the AV proportion of traffic is $r = v_a/v$ per (3). From the supply-demand equilibrium, each household of group j and type $i = \{a, r\}$ makes x_i^j trips such that

$$u(x_i^j) = \beta_i^j T(X), \qquad i = \{a, r\}, j \in J \tag{25}$$

where $T(X)$ is the travel time as a function of $X = \{x_i^j\}$. The utility of each household group j of vehicle type $i = \{a, r\}$ is U_i^j:

$$U_i^j = \int_0^{x_i^j} u(x)\mathrm{d}x - \beta_i^j x_i^j T(X) \qquad i = \{a, r\}, j \in J. \tag{26}$$

Social welfare, W, is the sum of utilities (26) weighted by the group size p^j and the household proportions N_a^j and N_r^j:

$$W = \sum_j p^j [N_a^j U_a^j + N_r^j U_r^j]. \tag{27}$$

We now derive the optimal social welfare for the power marginal utility function.

Proposition 6. *For a group $j \in J$, the adjusted capacity, $\bar{C}$, is maximized at the optimal AV traffic ratio, r^*, given by:*

$$r^* = \begin{cases} 1 & \dfrac{1}{2 - \tau(1+l)} \le \dfrac{c_a}{c_r} \qquad (28a) \\ 1 - \dfrac{c_a}{2(c_a - c_r)} + \dfrac{1}{2\tau(1+l) - 2} & \dfrac{1}{2 - \tau(1+l)} \le \dfrac{c_a}{c_r} < \dfrac{2\tau(1+l) - 1}{\tau(1+l)} \qquad (28b) \\ 0 & \dfrac{2\tau(1+l) - 1}{\tau(1+l)} > \dfrac{c_a}{c_r}\,. \qquad (28c) \end{cases}$$

The AV ratio in (28) maximizes $\hat{W}$, which is an approximate of the true social welfare W.

Proposition 6 extends Proposition 1 to the case of heterogeneous travelers. The qualitative results on the accuracy of the approximation are similar.

Note however that the unique AV ratio may be achievable by several different choices of $N_a^j, j \in J$. Hence, governing agencies can maximize social welfare as long as they regulate the optimal proportion of AVs in the network regardless of what group types are contributing to that level of automation. This observation follows from our assumptions that both the relocation load, l, and the time-cost ratios, $\beta_r^j/\beta_a^j = \tau$, are identical among all groups. If either one of these two conditions do not hold, then some specific groups within J should be chosen to make up the desired AV proportion of traffic. For example, if all τ values are identical among the households, then we should first choose to increase the automation level of the groups with a lower relocation load.

The discussion in Proposition 6 for heterogeneous users is equivalent to that of Proposition 1 for homogeneous users. The same three cases of social welfare per Fig. 3 still hold for heterogeneous users. Equation (28a) is Case I, (28b) is Case II, and (28c) is Case III.

5.2. Mode choice equilibrium for heterogeneous travelers

We now find the mode choice equilibrium of heterogeneous travelers. Let $N_a^{\circ j}$ be the AV household share of group j. The equilibrium $N_a^{\circ j}$ depends on the automation choices of all other groups denoted as N_a^{-j} where $-j = \{j' \in J \backslash j\}$. The two net utility functions of group j are defined as $B_i(N_a^j, N_a^{-j}), i = \{a, r\}$. According to Wardrop's two principles and per Proposition 5, an intermediate point $N_a^j \in (0, 1)$ is an equilibrium for group j if

$$B_a(N_a^j, N_a^{-j}) = B_r(N_a^j, N_a^{-j}), \tag{29}$$

contingent on the following stability test:

$$\frac{\mathrm{d}B_a(N_a^j, N_a^{-j})}{\mathrm{d}N_a^j} > \frac{\mathrm{d}B_r(N_a^j, N_a^{-j})}{\mathrm{d}N_a^j}, \tag{30}$$

which follows the same logic as (23).

The conditions in (29) and (30) imply that a best-response function for group j should consider the choices of the other groups. We denote the best response function of group j as $R^j(N_a^{-j})$ and define it via the following process: For a given set N_a^{-j}, we vary $N_a^j \in (0, 1)$ and check for the two conditions (29) and (30). If no such N_a^j is found, then we have an all-or-nothing solution, where $N_a^j = 1$ if $B_a(1, N_a^{-j}) \geq B_r(0, N_a^{-j})$ or $N_a^j = 0$ if $B_a(1, N_a^{-j}) < B_r(0, N_a^{-j})$.

The equilibrium point $N_a^{\circ j}$ is the intersection of the best-response function $R^j(N_a^{-j})$ of all groups $j \in J$. As the exact solution of this process does not lead to a closed form relation, we graphically present the heterogeneous mode choice equilibrium for two different scenarios.

Consider two groups of travelers. The first group has a large population size but a small time-cost: $p_1 = 0.67$, $p_2 = 0.33$, $\beta_r^1 = 1$, $\beta_r^2 = 1.4$, and $\beta_a^j = 0.8\beta_r^j$. That is, we consider a different time-cost ratios in both groups. The marginal utility function is $u(x) = 50x^{-1/3}$, and the travel time function is $T = (x/c)^3$ where c is the capacity with $c_a = 20, c_r = 10$. Both groups have

the same relocation load $l^1 = l^2 = 0.2$. In a second scenario we assume that the two groups have different time-cost ratios and relocation loads such that $\beta_r^1 = 1$, $\beta_r^2 = 1.4$, $\beta_a^1 = 0.8\beta_r^1$ and $\beta_a^2 = 0.75\beta_r^2$, and $l^1 = 0.8, l^2 = 0.3$.

In Fig. 6, we present the best response functions of both user groups, the socially optimal level of automation per (28), and the mode choice equilibrium solution where each household maximizes its own utility. In Fig. 6a, the socially optimal solution is a line that represents the optimal AV traffic ratio per (28). In contrast, the socially optimal solution in Fig. 6b, is a single point because the two groups have different time-cost ratios and relocation loads.

The mode choice equilibrium occurs at $N_a^1 = 0$ and $N_a^2 = 1$ in both scenarios, which is the intersect of the two best response functions. This mode choice equilibrium is closer to the socially optimal solution in Scenario 1 compared to Scenario 2.

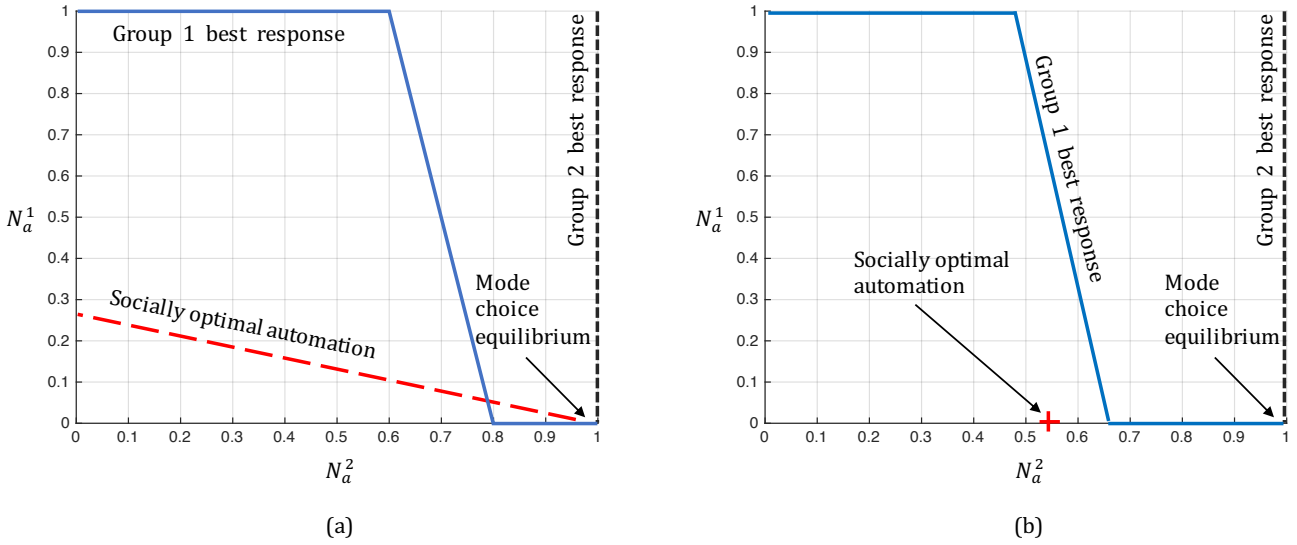

Figure 6: (a) Scenario 1: $l^1 = l^2 = 0.2$; $\beta_a^j = 0.8\beta_r^j$; (b) Scenario 2: $l^1 = 0.8, l^2 = 0.3; \beta_a^1 = 0.8\beta_r^1, \beta_a^2 = 0.75\beta_r^2$.

6. Simulation study of peer to peer sharing in Toronto

We present a simulation model of the City of Toronto. Our objective is twofold; to verify the analytical results using the simulation model and to present additional insights from the simulation model that were not possible to derive from the analytical model due to tractability issues. Specifically, we study the effects of the peer to peer sharing arrangements on social welfare and selfish adoption patterns. The simulation model is consistent with previous studies (Belavina et al., 2017; de Zegher et al., 2019).

The analytical model included simplifying assumptions that we relax in the simulation model. The simplifying assumptions include: lack of a network, homogeneous users, lack of a specific sharing model, and fixing an exogenous relocation load in the model that is exogenous and fixed.

In the simulation model, we present a network model and consider heterogeneity in the experienced travel time of users and their respective time costs. We also present a peer to peer sharing model where a coalition of households share a fleet of AVs. This model endogenizes the relocation load as a function of the properties of the sharing business model.

We first present the network of the simulation model in Section 6.1. We discuss the peer to peer sharing model in Section 6.2. We then present an iterative algorithm to find the AV and regular vehicle flows in Section 6.3, and the results in Section 6.4.

6.1. The network

We consider downtown Toronto as the case study. We obtain the demand data from the Transportation Tomorrow Survey (2019) that is collected every five years from residents of southern Ontario by the local and provincial government agencies. We obtain the network and other related data from the GTAModel V4.0 (2019). The network has 1228 links, 400 nodes and 491 origin-destination (OD) pairs. The length of the network is 256 km.

We consider the network $G(M, A)$ with a node set M and a link set A. Let $M_s \subset M$ and $M_e \subset M$ be the sets of origin and destination nodes, respectively. The network is connected and there is at least one path between each OD pair. Let S be the set of all (i, j) OD pairs where $i \in M_s$ and $j \in M_e$. We add superscripts "ij" to relate previously defined notation to OD pairs in S. For example, we denote the equilibrium shortest travel time for OD pair (i, j) by T^{ij}.

The maximum possible demand of (i, j) is D^{ij} vehicles per hour. We estimate this maximum demand as the observed demand in the dataset from the survey multiplied by an expansion factor of 1.5 or 2, e.g., for the expansion factor of 1.5 if the observed demand is 1000 vehicles per hour, we set the maximum demand to 1500 vehicles per hour.

We assume that a portion N_a^{ij} of travelers engages in peer to peer AV sharing and the remaining $N_r^{ij} = 1 - N_a^{ij}$ portion uses their own regular vehicle. The actual demand, denoted by d_k^{ij} with $k = \{a, r\}$, is sensitive to the OD travel time, T^{ij}, via the following exponential function, see e.g., the Transportation Tomorrow Survey (2019):

$$d_k^{ij} = N_k^{ij} D^{ij} \exp\left(-\alpha^{ij} \beta_k^{ij} T^{ij}\right) \qquad k = \{a, r\}. \tag{31}$$

For simplicity and tractability we use a single calibration parameter $\alpha^{ij} = \alpha$ and time cost $\beta_k^{ij} = \beta_k$ for all $(i, j) \in S$ and $k = \{a, r\}$. Specifically, we choose α for each expansion factor, such that the observed demand coincides with the resulting demand in our simulation model when no AVs are used. Specifically, for an expansion factor of 1.5 we obtained $\alpha = 0.65$ and for an expansion of 2, we obtained $\alpha = 0.71$. We use a time cost of $\beta_r = 20$ dollars per hour for regular households (the minimum hourly wage in Toronto until October 2020 is \$14, so about 50% higher seems sensible), and tested three different AV household time-costs of $\beta_a \in \{14, 16, 20\}$ dollars per

hour. The OD travel times, T^{ij}, are derived from the network model as explained below.

In addition to AV and regular vehicle traffic, we also have AV relocation traffic in the network. We observe that there is no point in (i) initially locating a vehicle in a node that is not an origin node (ii) relocating a vehicle to a non origin node, and (iii) relocating a vehicle from a non destination node. Therefore, the relocation loads are also generated only from origin nodes to destination nodes. We thus treat these also as (i, j) OD pairs (this may increase the set of OD pairs from the original one). We let "l" be the subscript that represents quantities that are related to this relocation load. We treat these relocation loads as demands over OD pairs and denote the relocation load between an (i, j) OD pair as d_l^{ij}. We derive the relocation loads that minimize the relocation traffic for a given demand on the network in Section 6.2.

We next aggregate the demand resulting from each OD pair to get a demand on every link of the network. Note that there may be more than one path connecting the (i, j) OD pair. Let P^{ij} indexed by $p \in P^{ij}$ be the set of all possible paths of (i, j), and let $P = \cup_{(i,j)} P^{ij}$ be the set of all paths. For the (i, j) OD pair the flow of type $k = \{a, r, l\}$ on path $p \in P^{ij}$ is denoted by $q_k^{ij,p}$. Thus, the sum of path flows is equal to the demand of each OD pair such that

$$d_k^{ij} = \sum_{p \in P^{ij}} q_k^{ij,p} \qquad\qquad k = \{a, r, l\}. \tag{32}$$

For every link $(u, v) \in A$ (note that (i, j) relates to an OD pair while (u, v) relates to a link) the AV, regular vehicle, and relocation flows are q_a^{uv}, q_r^{uv}, and q_l^{uv}. Let $\delta^{uv,p}$ be a binary parameter equal to one if link (u, v) is a link on path p. We aggregate the path flows into link flows as

$$q_k^{uv} = \sum_{(i,j) \in S} \sum_{p \in P^{ij}} q_k^{ij,p} \delta^{uv,p} \qquad\qquad k = \{a, r, l\}. \tag{33}$$

We denote total flow on link (u, v) by $q^{uv} = q_r^{uv} + q_a^{uv} + q_l^{uv}$. Similar to (3), the proportion of AVs on link (u, v) is:

$$r^{uv} = \frac{q_a^{uv} + q_l^{uv}}{q^{uv}}. \tag{34}$$

Let c_a^{uv} and c_r^{uv} be the AV and regular vehicle capacities of link (u, v), respectively. Similar to (4), we assume the capacity of link (u, v) is

$$c^{uv} = c_r^{uv} + r^{uv}(c_a^{uv} - c_r^{uv}). \tag{35}$$

We obtain the regular vehicle capacities for each link, c_r^{uv}, from the dataset and consider an AV capacity of $c_a^{uv} = 1.4 c_r^{uv}$ as in Chen et al. (2017b).

We obtain the travel time of link (u, v), denoted by t^{uv}, using the classic BPR function (as a

slightly modified version of (5)):

$$t^{uv} = t_0^{uv}\big(1 + a(\frac{q^{uv}}{c^{uv}})^b\big), \tag{36}$$

where t_0^{uv} is the free-flow travel time of link (u, v), and c^{uv} is obtained from (35). We use GTAModel V4.0 (2019) for the values the free-flow travel times, the constants of (36) ($a = 0.15$ and $b = 4$).

Under the network user equilibrium conditions, the travel time from origin node i to destination node j is the travel time of the shortest path (Patriksson, 2015):

$$T^{ij} = \min_{p \in P^{ij}} \sum_{(u,v)} t^{uv} \delta^{uv,p}. \tag{37}$$

The equilibrium traffic balances the travel times in (37) with the demands in (31). In Section 6.3, we present an algorithm that iterates between these until an equilibrium point is reached.

6.2. Peer to peer sharing model

Consider a peer to peer sharing model where n households share m AVs. As before, we assume that a portion N_a^{ij} of travelers create coalitions and share a fleet of AVs, while the remaining $N_r^{ij} = 1 - N_a^{ij}$ travelers use their personally owned regular vehicle. The cost of the AV is equally divided between the members of the coalition; if an AV costs F_a dollars, each household pays $f_a = mF_a/n$. Sharing a vehicle is possible because the AVs can self-relocate between multiple user requests. The relocation process, however, leads to zombie trips.

Assume that a fraction z^{ij} (which we call the availability parameter) of the demand on OD pair (i, j) has direct access to an AV. The remaining fraction $1 - z^{ij}$ has to wait for AVs to be relocated from a neighbouring node (dropped off by users that have arrived at their destinations or satisfied by zombie trips) to the origin node i. Moreover, we assume that the n households of each coalition are distributed proportional to demands, e.g., if the total demand is d_a^{ij}, then the demand for each coalition is d_a^{ij}/n. While in practice, coalitions may be formed among members with common origin or destination nodes, we leave it for future research to investigate the impact of geographical-based coalitions on the equilibrium usage rates.

Recall that d_l^{ij} is the relocation load from destination node $i \in M_e$ to origin node $j \in M_s$. We let $d_l^{ij}(n)$ be the relocation load of each coalition of size n. Given z^{ij}, the following assignment problem minimizes the total travel time of the relocation flows in the network:

$$\min_{d_l^{ij} \geq 0} \quad \sum_{ij} T^{ij} d_l^{ij}(n) \tag{38a}$$

$$\text{s.t.} \quad \sum_{j \in M_s} d_l^{ij}(n) \leq \sum_{j \in M_s} d_a^{ji} z^{ji}/n, \qquad \forall i \in M_e \tag{38b}$$

$$\sum_{i \in M_e} d_l^{ij}(n) = \sum_{i \in M_e} d_a^{ji}(1 - z^{ji})/n, \qquad \forall j \in M_s \tag{38c}$$

where (38a) minimizes the total relocation travel time, (38b) ensures that the relocation flow leaving each node is lower than the flow of the available fleet (arriving to this node), and (38c) ensures that relocation flows serve all users that do not have immediate access to AVs. We note that in (38), when $i = j$ the relocation trip is equivalent to an AV dropped off by one user and picked up by another user at the same node. These re-allocations take 0 time.

From the solution of (38), we derive the total relocation load as

$$d_l^{ij} = n d_l^{ij}(n). \tag{39}$$

We use Little's Law to derive the fleet size of each coalition as:

$$m = \sum_{ij} (d_l^{ij}(n) + d_a^{ij}/n) T^{ij}. \tag{40}$$

The availability factor z^{ij} directly influences the fleet size. A larger z^{ij} increases the part of the fleet directly accessed by users, $T^{ij} d_a^{ij}/n$, but decreases the fleet size in relocation, $T^{ij} d_l^{ij}(n)$. The AV households can choose z^{ij} to minimize the required fleet size while ensuring an acceptable level of service (in terms of waiting time). For simplicity, in (38) we consider a fixed availability parameter for all destination-origin points, i.e., $z^{ij} = z$. Note that the assignment problem (38) is infeasible if z is too small. The minimum acceptable value of $z = 0.5$ such that half of the AV users gain direct access and the other half wait until an AV becomes available. We note that as the coalition size increases reserving AVs becomes more challenging. Thus, coalition members may require a larger availability factor, z, before committing to a larger coalition.

6.3. The algorithm and performance measures

We present the following algorithm to find $\{q_a^{uv}, q_r^{uv}, q_l^{uv}\}$ as a function of the time-costs, β_a and β_r, calibration parameter, α, link capacities, c_r^{uv} and c_a^{uv}, maximum demands, D^{ij}, availability factor, z, and the automation level, N_a. We assume all these are exogenous; their values are given or derived as explained above. We use a convergence parameter $\eta = 0.01$. For simplicity of the exposition we only include parenthesis to relate quantities to the iteration in which they were calculated in the stopping rules, e.g., $q^{uv}(y)$ is the traffic of link (u, v) at iteration y.

1. *Initiate* [Outputs = $\{c^{uv}, T^{ij}\}$]

Set the iteration count $s = 1$, the demands $d_k^{ij} = 0$ for all (i, j) OD pairs, $k = \{a, r, l\}$, and link capacities as $c^{uv} = c_r^{uv}$. Find the travel times T^{ij} for all (i, j) OD pairs with a shortest path algorithm where given (36), $t^{uv} = t_0^{uv}$.

2. *Demand* [Inputs = $\{T^{ij}\}$; Outputs = $\{d_a^{ij}, d_r^{ij}\}$]
For $k = \{a, r\}$ and all OD pairs (i, j), calculate the AV and regular vehicle demands from (31) and label them as $\hat{d}_k^{ij}$. Update demands for each (i, j) OD pair using the Mean of Successive Averages algorithm (Patriksson, 2015) as

$$d_k^{ij} := \frac{(s-1)d_k^{ij}}{s} + \frac{\hat{d}_k^{ij}}{s}, \tag{41}$$

and increase the iteration counter $s := s + 1$.

3. *Relocation load* [Inputs = $\{T^{ij}, d_a^{ij}\}$; Outputs = $\{d_l^{ij}\}$]
Solve (38) to find the relocation load d_l^{ij} for each (i, j) OD pair. Set a second iteration counter $y = 1$ and all link flows $q_k^{uv} = 0$.

4. *Traffic Assignment* [Inputs = $\{c^{uv}, d_r^{ij}, d_a^{ij}, d_l^{ij}\}$; Outputs = $\{q_a^{uv}, q_r^{uv}, q_l^{uv}, T^{ij}\}$]
For each link (u, v) calculate the link travel time using the BPR function of (36). For each OD pair (i, j) find the shortest path with travel time T^{ij} per (37). Assign demands d_k^{ij} to the shortest path and use (33) to calculate the link flows $\hat{q}_k^{uv}$. Use the Mean of Successive Averages algorithm (Patriksson, 2015) to update the link flows as

$$q_k^{uv} := \frac{(y-1)q_k^{uv}}{y} + \frac{\hat{q}_k^{uv}}{y}, \tag{42}$$

and increase the iteration counter $y := y + 1$.

5. *Link Capacity* [Inputs = $\{q_a^{uv}, q_r^{uv}, q_l^{uv}\}$; Outputs = $\{c^{uv}\}$]
Update the AV proportions on each link using (34). Calculate the link capacities from (35). If $\dfrac{\max(q^{uv}(y) - q^{uv}(y-1))}{q^{uv}(y-1)} \leq \eta$ for all k, then go to Step 6, otherwise, go to Step 4.

6. *Terminate*: If $\dfrac{\max(d_k^{ij}(s) - d_k^{ij}(s-1))}{d_k^{ij}(s-1)} \leq \eta$ for all k and (i, j) OD pair, then stop, otherwise go to Step 2.

Based on the results of the algorithm we analyze the following performance measures. The expected waiting time given waiting (i.e., waiting of customers that did not pick up an AV initially allocated to their origin node)

$$WT = \frac{\sum_{(i,j)\in S} d_l^{ij}(n) T^{ij}}{\sum_{(i,j)\in S} d_l^{ij}(n)}, \tag{43}$$

the total AV fleet size (based on Little's Law)

$$FL = \sum_{(i,j)\in S} (d_l^{ij} + d_a^{ij}) T^{ij}, \tag{44}$$

the expected relocation load ratio per AV trip as

$$l = \frac{\sum_{(i,j)\in S} d_l^{ij}}{\sum_{(i,j)\in S} d_a^{ij}}, \tag{45}$$

the net utility of AV and regular households as in (8)

$$B_k = \sum_{(i,j)\in S} \int_0^{d_k^{ij}} D^{ij} \exp\left(\alpha\beta_k T^{ij}\right) - \beta_k d_k^{ij} T^{ij} - f_k \qquad k = \{a, r\}, \tag{46}$$

and the social welfare

$$W = \sum_{k=\{a,r\}} \sum_{(i,j)\in S} \int_0^{d_k^{ij}} D^{ij} \exp\left(\alpha\beta_k ij T^{ij}\right) - \beta_k^{ij} d_k^{ij} T^{ij}. \tag{47}$$

6.4. Simulation findings

We present the results of the simulation model. Note that for brevity, we only report results for an expansion factor of 1.5 (we observed similar qualitative results for a factor of 2). We validate the findings of the analytical model in Section 6.4.1, then investigate the effect of the coalition size in a peer to peer sharing model on the performance measures discussed in Section 6.4.2.

We assume that all OD pairs have the same proportion of AV households, i.e., $N_a^{ij} = N_a$ for all $(i, j) \in S$. We run the model at varying automation levels of $N_a \in \{0, 0.05, ..., 1\}$. We also vary the ratio $\beta_r/\beta_a \in \{1, 1.25, 1.4\}$ and discuss in Appendix B the heterogeneous case where the ratio is unique for each (i, j) OD pair.

6.4.1. Validation of the analytical model

In Fig. 7, we present four measures of effectiveness under varying time-cost ratios, $\beta_r/\beta_a \in \{1, 1.25, 1.4\}$, and levels of automation, $N_a = \{0, 0.05, ..., 1\}$.

In Fig. 7a-c, we present the **net utility** of the AV and regular households for coalition size $n = 1$ from (46). In all three cases, the utilities do not intersect implying that the selfish decision of all households is to use AVs. Because the utilities do not intersect, the full-automation decision is also stable according to Proposition 5. Moreover, in all three cases the household utilities nearly double from no automation to full automation. We set the amortized vehicle ownership costs as $f_r = 10$ and $f_a = 30$.

In Fig. 7d we depict the **social welfare** from (47). The social welfare for $\beta_r/\beta_a = 1.4$ corresponds to Case I, which recommends full automation, whereas the social welfare for $\beta_r/\beta_a \in \{1, 1.25\}$ corresponds to Case IIa, which recommends partial automation.

From Fig. 7d we further observe that the **optimal level of automation**, N_a^*, first decreases from $N_a^* = 0.79$ (at $\beta_r/\beta_a = 1$) to $N_a^* = 0.61$ (at $\beta_r/\beta_a = 1.25$) then increases to $N_a^* = 1$ (at

$\beta_r/\beta_a = 1.4$). The initial decrease is due to the additional demand and congestion caused by AVs, and the latter increase is due to the capacity effects of AVs. This decrease and increase is consistent with Proposition 2.

We observe from comparing the social welfare with the household utilities that the optimal level of automation at $\beta_r/\beta_a = 1.4$ is equivalent to the selfish adoption pattern of households, i.e., $N_a^\circ = N_a^* = 1$. In contrast, for $\beta_r/\beta_a = \{1, 1.25\}$, we have $N_a^\circ > N_a^*$. Thus, the selfish adoption patterns prohibit from reaching the maximum possible social welfare.

In Fig. 7e, we present the **relocation load** calculated from (45). When N_a is close to zero, the highest relocation load occurs at $\beta_r/\beta_a = 1.4$ (the highest time cost ratio) because of the larger demand at this time cost ratio. However, when N_a is close to one, the relocation load is lowest at $\beta_r/\beta_a = 1.4$ because the increased demand creates efficient routes for relocating the AVs. From Fig. 7e, we also show that the relocation load is fairly robust with N_a in agreement with Assumption 1 of the analytical model.

In Fig. 7f we depict the **expected waiting time** from (43). As expected, this waiting time increases with N_a for all time-cost ratios. The waiting times are in order of 5 to 9 minutes. We note the difference in the waiting time of the simulation model and the analytical model discussed in Appendix C. In the analytical model we determine the fleet size required to keep the expected waiting time below an exogenously given service level threshold. In the simulation model we calculate the expected waiting time of the system based upon the exogenous availability factor z. The peer to peer sharing coalitions can reduce waiting by increasing z (i.e., providing more direct access to AV as opposed to relocating AVs).

6.4.2. Insights on peer to peer sharing of AVs

We now discuss the properties of the peer to peer sharing and how these are impacted by the **coalition size**. For this we let the coalition size be $n \in \{1, 2..., 10\}$.

In Fig. 8a, we depict the **social welfare** at three levels of automation $N_a = \{0.1, .0.5, 0.9\}$. The coalition size has a higher effect on social welfare at larger levels of automation. The effect of the coalition size on social welfare wears down at larger n because the efficient relocation routes are already exploited. Moreover, at the lowest automation level, $N_a = 0.1$, the coalition size has a marginal impact on social welfare because there are not enough AV users to effect the level of traffic on roads.

In Fig. 8b, we present the **relocation load**. The coalition size n reduces the relocation load due to the increased efficiency of relocating vehicles. However, this effect also wears down at larger n similar to Fig. 8a. We also observe that the relocation load ratios are not significantly affected by the automation levels. This shows that the relocation load and demand increase proportionally w.r.t. the automation level. The largest relocation ratio is 0.48 which means that about half of the AVs are making zombie trips in the network.

In Fig. 8c, we present the total **fleet size** from (44). The coalition size has a higher impact on the fleet size at the highest level of automation of $N_a = 0.9$. Moreover, the fleet size increases with the level of automation due to increased demand of AV households. Also the fleet size for a given level of automation is not sensitive to the size of the coalition.

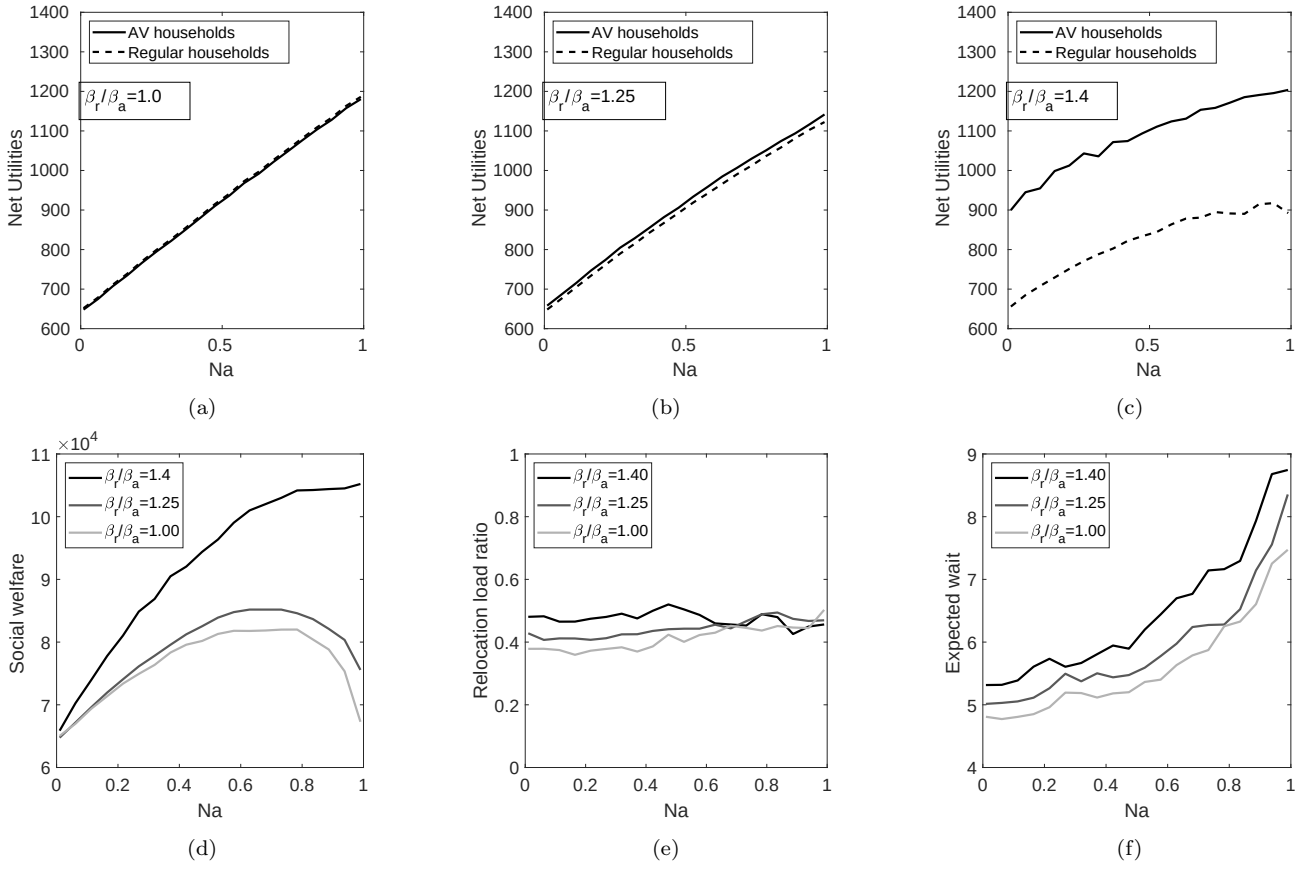

Figure 7: Simulation results at varying time-cost ratios. Parameters are from the GTAModel V4.0 (2019) and the Transportation Tomorrow Survey (2019). (a)-(c) Household net utility, (d) social welfare, (e) relocation load ratio, and (d) expected wait.

7. Conclusions

Autonomous vehicles promote shared mobility because they can be relocated among multiple passengers in driverless mode. By sharing a fleet of AVs, each user pays less for mobility and has a higher incentive to travel. This can potentially lead to more traffic, which can be instrumental in urban areas. On the upside, however, connectivity of AVs allow them to use roads more efficiently. Hence, the extra traffic from automation may not increase congestion. This trade-off between infrastructure efficiency and the induced traffic has caused a debate about the benefits of vehicle automation. Experts are taking sides based on speculations without substantial scientific evidence based on real data. This is partially because AVs are not yet commercialized, and no data is available to support each side's arguments. In the absence of data, analytical methods

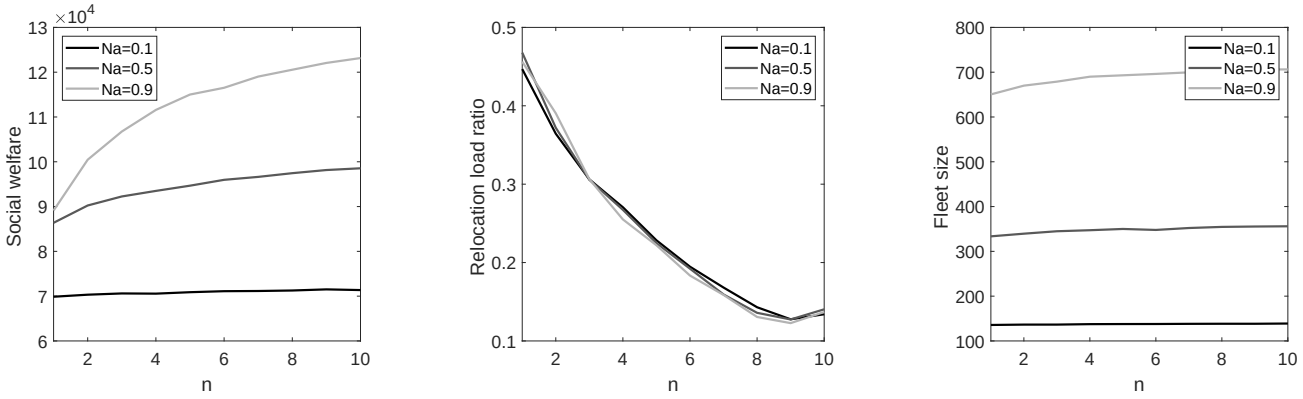

Figure 8: Simulation results at varying coalition size n. Parameters are from the GTAModel V4.0 (2019) and the Transportation Tomorrow Survey (2019).

that give insight on vehicle automation in different operating scenarios can be very useful. This paper presents one of the first analytical approaches to provide such insights.

We address the automation controversy using analysis based on supply-demand curves. We capture the impact of automation on the supply-demand equilibrium and derive several insights. A major conclusion is that we cannot blindly support or dispute automation without the knowledge of (i) the transportation infrastructure, and (ii) the vehicle-sharing behavior of consumers. According to these two factors, one of three cases can occur. The first stipulates that any level of automation is always beneficial, thus supporting the advocate's side of the debate. In the second, partial automation is optimal, and in the third, no vehicles should be automated. Hence, cities must not inadvertently support AVs without an in-depth analysis of their impacts.

We derive several insights. First, while it is commonly accepted that any increase in traffic will lead to longer travel times, we show that this may not be the case in the presence of AVs. It is possible to increase traffic and experience a shorter travel time under automation. Second, as the level of comfort of AVs increases as users can engage in useful activities while traveling, automation becomes more harmful to social welfare. Such a larger decrease in social welfare results from the tendency of AV owners to travel more and increase traffic. Hence, cities should refrain from excessive automation when the comfort level increases.

There are many avenues for future research on vehicle automation. An important next step is to investigate the pricing structure of households in each AV coalition (joint owners of AVs); how should the ownership costs be equitably divided among the members of each coalition to reach an equilibrium where no household benefits from switching to another coalition. A cooperative game theory approach can then be used to derive the equilibrium. Moreover, while AVs are expected to benefit the society in many ways, their high initial ownership cost may hinder their widespread adoption. Therefore, government intervention is instrumental to ensure that AVs are affordable

for the public at the right level. Policies that endorse automation may use subsidization, taxation, or promotion of vehicle sharing between multiple users. Other influential policies include changes in traffic rules, taxi regulation, and land use changes. Research in these areas could allow us to better comprehend the impacts of vehicle automation in the future and provide further tools for policymakers to make better decisions.

References

Allahviranloo, M., Chow, J. Y., 2019. A fractionally owned autonomous vehicle fleet sizing problem with time slot demand substitution effects. Transportation Research Part C: Emerging Technologies 98, 37–53.

Allen, K., 2017. Uber's self-driving cars hit toronto streets — in manual mode.
URL thestar.com

Antweiler, W., 2018. The virtues of negative exponential demand.
URL https://wernerantweiler.ca/blog.php?item=2018-06-30.

Atiyeh, C., 2012. Predicting traffic patterns, one honda at a time.

Audi, 2016. Audi launches first vehicle-to-infrastructure (v2i) technology in the u.s. starting in las vegas.
URL https://www.audiusa.com/newsroom/news/press-releases/

Avci, B., Girotra, K., Netessine, S., 2014. Electric vehicles with a battery switching station: Adoption and environmental impact. Management Science 61 (4), 772–794.

Bansal, P., Kockelman, K. M., 2017. Forecasting americans' long-term adoption of connected and autonomous vehicle technologies. Transportation Research Part A: Policy and Practice 95, 49–63.

Belavina, E., Girotra, K., Kabra, A., 2017. Online grocery retail: Revenue models and environmental impact. Management Science 63 (6), 1781–1799.

Bellos, I., Ferguson, M., Toktay, L. B., 2017. The car sharing economy: Interaction of business model choice and product line design. Manufacturing & Service Operations Management 19 (2), 185–201.

Benjaafar, S., Hu, M., 2019. Operations management in the age of the sharing economy: What is old and what is new? Forthcoming, Manufacturing and Service Operations Management.

Benjaafar, S., Kong, G., Li, X., Courcoubetis, C., 2018. Peer-to-peer product sharing: Implications for ownership, usage, and social welfare in the sharing economy. Management Science.

Bloomberg, 2017. Initiatives on cities and autonomous vehicles.
URL https://avsincities.bloomberg.org/

Buck, R. C., 2003. Advanced calculus. Waveland Press.

Button, K., 2010. Transport economics. Edward Elgar Publishing.

Chen, D., Ahn, S., Chitturi, M., Noyce, D. A., 2017a. Towards vehicle automation: Roadway capacity formulation for traffic mixed with regular and automated vehicles. Transportation Research Part B: Methodological 100, 196–221.

Chen, T. D., Kockelman, K. M., Hanna, J. P., 2016a. Operations of a shared, autonomous, electric vehicle fleet: implications of vehicle & charging infrastructure decisions. Transportation Research Part A,(under review for publication).

Chen, Z., He, F., Yin, Y., Du, Y., 2017b. Optimal design of autonomous vehicle zones in transportation networks. Transportation Research Part B: Methodological 99, 44–61.

Chen, Z., He, F., Zhang, L., Yin, Y., 2016b. Optimal deployment of autonomous vehicle lanes with endogenous market penetration. Transportation Research Part C: Emerging Technologies 72, 143–156.

City Lab, 2017. The future of autonomous vehicles is shared.
URL http://citylab.com/

Cohen, M. C., Lobel, R., Perakis, G., 2015. The impact of demand uncertainty on consumer subsidies for green technology adoption. Management Science 62 (5), 1235–1258.

Daganzo, C. F., 2010. Public transportation systems: Basic principles of system design. Operations Planning and Real-Time Control.

de Oliveira, Í. R., 2017. Analyzing the performance of distributed conflict resolution among autonomous vehicles. Transportation Research Part B: Methodological 96, 92–112.

de Zegher, J. F., Iancu, D. A., Lee, H. L., 2019. Designing contracts and sourcing channels to create shared value. Manufacturing & Service Operations Management 21 (2), 271–289.

Economist, 2016. The driverless, car-sharing road ahead January.

Fagnant, D. J., Kockelman, K., 2015. Preparing a nation for autonomous vehicles: opportunities, barriers and policy recommendations. Transportation Research Part A: Policy and Practice 77, 167–181.

Forbes, 2018. The link between autonomous vehicles and blockchain.
URL https://www.forbes.com/sites/geraldfenech/

Ford Media, 2017. Ford targets fully autonomous vehicle for ridesharing in 2021; investment in new tech companies, doubles silicon valley team.
URL http://media.ford.com/

GTAModel V4.0, 2019.
URL https://tmg.utoronto.ca/doc/1.4/gtamodel/index.html

Harper, C. D., Hendrickson, C. T., Mangones, S., Samaras, C., 2016. Estimating potential increases in travel with autonomous vehicles for the non-driving, elderly and people with travel-restrictive medical conditions. Transportation Research Part C: Emerging Technologies 72, 1–9.

Hassin, R., Haviv, M., 2003. To queue or not to queue: Equilibrium behavior in queueing systems. Vol. 59. Springer Science & Business Media.

He, L., Mak, H.-Y., Rong, Y., Shen, Z.-J. M., 2017. Service region design for urban electric vehicle sharing systems. Manufacturing & Service Operations Management 19 (2), 309–327.

Hensley, R., 2009. Electrifying cars: how three industries will evolve. McKinsey Quart.

Hu, M., 2019. Sharing economy: making supply meet demand. Springer.

Huang, J., Leng, M., Parlar, M., 2013. Demand functions in decision modeling: A comprehensive survey and research directions. Decision Sciences 44 (3), 557–609.

Little, J. D., 2011. OR Forum-Little's Law as viewed on its 50th anniversary. Operations research 59 (3), 536–549.

Mahmassani, H. S., 2016. 50th anniversary invited article - autonomous vehicles and connected vehicle systems: Flow and operations considerations. Transportation Science 50 (4), 1140–1162.

Martin, E., Shaheen, S., 2016. Impacts of car2go on vehicle ownership, modal shift, vehicle miles traveled, and greenhouse gas emissions: an analysis of five north american cities. Transportation Sustainability Research Center, UC Berkeley.

Mersky, A. C., Samaras, C., 2016. Fuel economy testing of autonomous vehicles. Transportation Research Part C: Emerging Technologies 65, 31–48.

Muoio, D., 2017. Self-driving cars could be terrible for traffic — here's why.
URL http://www.businessinsider.com/self-driving-cars-traffic-congestion-2017-6/

National Highway Traffic Safety Administration, 2013. Preliminary statement of policy concerning

automated vehicles. washington, d.c.
Nourinejad, M., 2018. Economics of parking: Short, medium, and long-term planning. Ph.D. thesis.
Nourinejad, M., Roorda, M. J., 2018. Cruising for parking in the era of autonomous vehicles.
Ortuzar, J. d. D., Willumsen, L. G., 2002. Modelling transport. Vol. 3.
Patriksson, M., 2015. The traffic assignment problem: models and methods. Courier Dover Publications.
Petruzzi, N. C., Dada, M., 1999. Pricing and the newsvendor problem: A review with extensions. Operations research 47 (2), 183–194.
Ray, S., Li, S., Song, Y., 2005. Tailored supply chain decision making under price-sensitive stochastic demand and delivery uncertainty. Management Science 51 (12), 1873–1891.
Raz, G., Ovchinnikov, A., 2015. Coordinating pricing and supply of public interest goods using government rebates and subsidies. IEEE Transactions on Engineering Management 62 (1), 65–79.
Seo, T., Asakura, Y., 2017. Endogenous market penetration dynamics of automated and connected vehicles: Transport-oriented model and its paradox.
Shchetko, N., 2014. Laser eyes pose price hurdle for driverless cars. Wall Street Journal.
Tian, L., Jiang, B., 2017. Effects of consumer-to-consumer product sharing on distribution channel. Production and Operations Management.
Transportation Tomorrow Survey, 2019.
URL `http://www.transportationtomorrow.on.ca/`
Vox, 2017. Unless we share them, self-driving vehicles will just make traffic worse. David, Roberts.
Wardrop, J. G., 1952. Road paper. some theoretical aspects of road traffic research. Proceedings of the institution of civil engineers 1 (3), 325–362.
Washington Post, 2018. Gm launches a peer-to-peer car-sharing service.
URL `https://www.washingtonpost.com/technology/`
Waymo, 2016. On the road.
URL `https://waymo.com/ontheroad/`
Yang, B., Monterola, C., 2016. Efficient intersection control for minimally guided vehicles: A self-organised and decentralised approach. Transportation Research Part C: Emerging Technologies 72, 283–305.
Zhu, F., Ukkusuri, S. V., 2015. A linear programming formulation for autonomous intersection control within a dynamic traffic assignment and connected vehicle environment. Transportation Research Part C: Emerging Technologies 55, 363–378.

Appendix A: Proof of propositions

Proof of Lemma 1: Comparing the two equilibrium conditions from (6), we get

$$u(x_r^*) = u(x_a^*)\frac{\beta_r}{\beta_a}. \tag{48}$$

Taking the inverse of (48), we get (10).

For the power marginal utility function, the inverse function is $u^{-1}(x) = x^{-\gamma}$. Hence, we can rewrite (10) as $x_r^* = \left(x_a^{*-1/\gamma}(\beta_r/\beta_a)\right)^{-\gamma}$, which is simplified to (11).

Proof of Proposition 1: We establish (22) by showing first that the approximate social

welfare, $\hat{W} = U_a$ in (20), and the adjusted capacity increase/decrease monotonically together. Therefore, given (49, satisfying the first-order-conditions for optimizing U_a w.r.t. N_a is equivalent to satisfying them for optimizing $\bar{C}$ w.r.t. N_a. Then, because both functions have a finite number of extreme points ($\bar{C}$ is a concave function defined on a convex set $N_a \in [0,1]$), the first-order-conditions for maximizing U_a (or U_r) and $\bar{C}$ are satisfied by the same $\hat{N}_a^*$.

According to the chain rule, we have

$$\frac{\mathrm{d}U_a}{\mathrm{d}N_a} = \frac{\mathrm{d}U_a}{\mathrm{d}\bar{C}} \frac{\mathrm{d}\bar{C}}{\mathrm{d}N_a}, \tag{49}$$

where

$$\frac{\mathrm{d}U_a}{\mathrm{d}\bar{C}} = \frac{\mathrm{d}U_a}{\mathrm{d}x_a^*} \frac{\mathrm{d}x_a^*}{\mathrm{d}\bar{C}} + \frac{\mathrm{d}U_a}{\mathrm{d}T} \frac{\mathrm{d}T}{\mathrm{d}\bar{C}}. \tag{50}$$

Moreover, the first-order-conditions w.r.t. x_a^* imply that $\mathrm{d}U_a/\mathrm{d}x_a^* = 0$, so that

$$\frac{\mathrm{d}U_a}{\mathrm{d}\bar{C}} = \frac{\mathrm{d}U_a}{\mathrm{d}T} \frac{\mathrm{d}T}{\mathrm{d}\bar{C}} > 0, \tag{51}$$

where the inequality follows because the travel time, T, decreases with the adjusted capacity, $\bar{C}$, and $\mathrm{d}U_a/\mathrm{d}T < 0$.

We next show that the adjusted capacity satisfies the second-order-condition and $\hat{N}_a^*$ from (22b) is its maximizer. Evaluating the second derivative of $\bar{C}$ at the optimal $\hat{N}_a^*$ from (22b), we have

$$\frac{\mathrm{d}^2\bar{C}}{\mathrm{d}N_a^2} = -\frac{\Big(\tau(1+l)-1\Big)\Big(c_a(1+l)\tau - c_r\Big)^4}{8(c_a-c_r)^3(1+l)^3\tau^3} < 0, \tag{52}$$

establishing that $\hat{N}_a^*$ in (22b) maximizes $\bar{C}$ and thus U_a (and U_r).

We next assess the boundaries of $\hat{N}_a^*$ in (22a) and (22c). Specifically, for $\hat{N}_a^* \geq 1$, we have

$$\frac{1}{2-\tau(1+l)} \leq \frac{c_a}{c_r}.$$

Note that $\bar{C}$ is strictly concave when $1\Big(2-\tau(1+l)\Big) \leq c_a/c_r$ and $0 \leq N_a \leq 1$. Hence, $\hat{N}_a^* = 1$ is the unique maximizer of $\bar{C}$.

For $\hat{N}_a^* \leq 0$ in (22c) we have

$$\frac{2\tau(1+l)-1}{\tau(1+l)} \geq \frac{c_a}{c_r}.$$

Note that $\frac{\mathrm{d}\bar{C}}{\mathrm{d}N_a} < 0$ when $\frac{c_a}{c_r} \leq 1 + \frac{l}{1+l}$ and $0 \leq N_a \leq 1$. Hence, $\hat{N}_a^* = 0$ is the unique maximizer of $\bar{C}$.

Proof of Proposition 2: At $\tau = 1$, the optimal levels of automation of the approximate and the true social welfare are identical, i.e., N_a^* is given by (22). From the derivative of (22b) w.r.t.

τ at $\tau = 1$ we show

$$\frac{\partial N_a^*}{\partial \tau}|_{\tau=1} = -(1+l)\Big(\frac{c_r^2 + c_a^2(1+l)^2 - 2c_a c_r(1+l+l^2)}{l^2(c_a - c_r + c_a l)^2}\Big) < 0. \tag{53}$$

Observe that (53) is strictly negative as long as $\frac{c_a}{c_r} > \frac{1}{1+l+l^2-l\sqrt{2+l(2+l)}}$. From the bounds of (22b), (it is easy to verify that the equality holds for $l = 0$ and the function $(1 + 2l)/(1 + l)$ grows faster with l in this range) we know that $\frac{c_a}{c_r} \geq \frac{1+2l}{1+l}$ at $\tau = 1$. Because $\frac{1+2l}{1+l} \geq \frac{1}{1+l+l^2-l\sqrt{2+l(2+l)}}$ for $l \in [0, 1]$, we conclude that $\frac{c_a}{c_r} > \frac{1}{1+l+l^2-l\sqrt{2+l(2+l)}}$ and, thus, (53) is negative.

Moreover, at $\tau \to \infty$, from (18) we have $\lim_{\tau\to\infty} U_r/U_a = 0$; thus, $N_a^* = 1$ (intuitively, this follows because the AV time-cost is negligible). From these two boundary conditions (i.e., at $\tau = 1$ and when $\tau \to \infty$) and according to the Mean Value Theorem (Buck, 2003) there exists at least one $\hat{\tau} \in (1, \infty)$ such that $\frac{\partial N_a^*}{\partial \tau} = 0$. Thus, there exists a range within $(1, \hat{\tau})$ that N_a^* decreases with τ and a range within $(\hat{\tau}, \infty)$ where N_a^* increases with τ.

Proof of Proposition 3: At full and no automation, the social welfare is $W = U_a$ and $W = U_r$, respectively. For the power-utility function, the total utility at the equilibrium number of trips is (Antweiler, 2018):

$$U_i(x_i^*) = \frac{x_i^{*1-1/\gamma}}{\gamma - 1}, \qquad\qquad i = \{a, r\} \tag{54}$$

According to (16), given the free-flow travel time $T_0 = 0$, the equilibrium trips at full and no automation are $x_a^* = (\frac{c_a^b}{\beta_a(1+l)})^{\gamma/(1+b\gamma)}$ and $x_r^* = (c_r^b/\beta_r)^{\gamma/(1+b\gamma)}$, respectively. We use these x_i^* in (54) to derive the full-automation social welfare at $N_a = 1$ as $(c_a^b/\beta_a(1 + l)^b)^{(\gamma-1)/(b\gamma+1)}/(\gamma - 1)$, and the no automation social welfare at $N_a = 0$ as $(c_r^b/\beta_r)^{(\gamma-1)/(b\gamma+1)}/(\gamma - 1)$. According to both expressions, the social welfare at full-automation is larger than (or equal to) the social welfare at no-automation if $c_a/c_r \geq (1 + l)(\beta_a/\beta_r)^{1/b}$; Otherwise, the social welfare is smaller at full-automation compared to no-automation.

Proof of Proposition 4: We discuss each of the four scenarios.

Scenario 1: Let $f(\tau) = \frac{2\tau(1+l)-1}{\tau(1+l)}$. From (22c), Case III occurs when $c_a/c_r < f(\tau)$. Because $\lim_{\tau\to\infty} f(\tau) = 2$ and $\frac{\partial f(\tau)}{\partial \tau} > 0$ for any $\tau > 0$, we have an upper-bound of $\hat{f} = 2$ on $f(\tau)$. Thus, Case III does not happen when $c_a/c_r \geq 2$ because the condition (22c) is not satisfied for any τ.

Scenario 2: From (22a), Case I occurs if $c_a/c_r \geq \frac{1}{2-\tau(1+l)}$. When $\tau = 1$ (i.e., $\beta_r/\beta_a = 1$) and $l \to 1$ we have:

$$\lim_{l\to 1} \frac{1}{2 - (1 + l)} = \infty. \tag{55}$$

Thus, according to (55) and because the capacity ratio is finite (i.e., $c_a/c_r < \infty$), the condition in (22a) is never satisfied and Case I does not happen.

Scenario 3: Let $\beta_a = \beta_r$, thus $\tau = 1$ and with $l = 0$, in (22a), we have $c_a/c_r \geq 1$, which is

always true. Thus, according to (22a) only Case I can happen in this scenario.

Scenario 4: From (22a), Case I occurs if $c_a/c_r \geq \frac{1}{2-\tau(1+l)}$. When $\tau > 2$ (i.e., $\beta_r/\beta_a > 2^{1/\gamma}$), we have

$$\frac{1}{2-\tau(1+l)} < 0. \tag{56}$$

Thus, according to (56) and because $c_a/c_r > 0$, the condition in (22a) is never satisfied and Case I does not happen.

Proof of Proposition 5: For intermediate points $N_a^\circ \in (0,1)$, where $B_r(N_a^\circ) = B_a(N_a^\circ)$, we propose a stability test. Assume the instability condition in (23) is satisfied. If we increase N_a by $\mathrm{d}N_a$, then according to (23) we have $B_a(N_a + \mathrm{d}N_a) > B_r(N_a + \mathrm{d}N_a)$. Thus, $\mathrm{d}N_a$ new autonomous households gain a higher net utility and are satisfied with changing their mode. Similarly, if we decrease N_a by $\mathrm{d}N_a$, then according to (23) we have $B_a(N_a + \mathrm{d}N_a) < B_r(N_a + \mathrm{d}N_a)$. Thus, $\mathrm{d}N_a$ new regular households households gain a higher net utility than before and are satisfied with their change of mode. The same analysis applies to regular households, because decreasing (increasing) N_a is analogous to increasing (decreasing) N_r. A similar argument shows that if the opposite of (23) holds, the equilibrium is unstable.

We now discuss the existence and uniqueness of the equilibrium solution. In Case I, B_a and B_r are both increasing w.r.t. N_a. Thus, they intersect at most once. If they do not intersect at all, then we have a unique boundary solution (with the boundary condition $B_a(1) \neq B_r(0)$). If they do intersect, then we have an unstable mid-point equilibrium because of (23); thus, there is only a single stable equilibrium at the boundary. A similar reasoning proves the existence and uniqueness of the stable equilibrium in Case III.

Now consider Case II. We know that B_a and B_r are maximized at the same $\hat{N}_a^*$ because $U_a/U_r = (\beta_r/\beta_a)^{\gamma-1}$. For $N_a \leq \hat{N}_a^*$, B_a and B_r can intersect at most once, which, upon existence, is unstable because of (23). In contrast, for $N_a > \hat{N}_a^*$, B_a and B_r can intersect at most once, which, upon existence, is a stable equilibrium. Thus, there exists a unique equilibrium point N_a° that satisfies $N_a^\circ \geq \hat{N}_a^*$. If B_a and B_r do not intersect, then we have a unique all-or-nothing assignment (with the boundary condition $B_a(1) \neq B_r(0)$).

Proof of Proposition 6: For a power-type marginal utility function, we use Lemma 1 to derive group j trips as

$$x_a^j = x_r^j(\beta_r^j/\beta_a^j)^\gamma \qquad\qquad i = \{a, r\}, j \in J, \tag{57}$$

where $\gamma > 1$ is a parameter.

More generally, from the system of equilibrium equations (25), the household trips of every

two groups $j, j' \in J$ are related so that

$$x_i^j = x_{i'}^{j'}(\beta_{i'}^{j'}/\beta_i^j)^\gamma \qquad\qquad i, i' = \{a, r\}, j, j' \in J. \tag{58}$$

Using (58), we need only one x_i^j to derive the vector $X = \{x_i^j\}$. We consider a reference AV household group $j = 1$ $i = a$, such that (58) becomes $x_i^j = x_a^1(\beta_a^1/\beta_i^j)^\gamma$ where $i = \{a, r\}, j \in J$. We use this condition to rewrite the AV trip volume in (24) as

$$v_a = x_a^1 \sum_j p^j N_a^j (\beta_a^1/\beta_a^j)^\gamma (1 + l), \tag{59}$$

and, the regular vehicle traffic volume becomes

$$v_r = x_a^1 \sum_j p^j N_r^j (\beta_a^1/\beta_r^j)^\gamma. \tag{60}$$

Given $v = v_a + v_r$, $r = v_a/v$, $c = c_r + (c_a - c_r)r$, the travel time function is

$$T = T_0 + (\frac{x_a^1}{\bar{C}})^b, \tag{61}$$

where $\bar{C}$ is the adjusted capacity defined initially at (15) and is rewritten as:

$$\bar{C} = \frac{c_a \sum_j p^j N_a^j (\beta_a^1/\beta_a^j)^\gamma (1 + l) + c_r \sum_j p^j N_r^j (\beta_a^1/\beta_r^j)^\gamma}{\Big(\sum_j p^j N_a^j (\beta_a^1/\beta_a^j)^\gamma (1 + l) + \sum_j p^j N_r^j (\beta_a^1/\beta_r^j)^\gamma \Big)^2} \tag{62}$$

Similar to Proposition 1, we present the following upper-bound on social welfare defined as $\hat{W} = \sum_j p^j U_a^j$. Then, one can use the same process as of Proposition 1 to show that $\hat{W}$ and the $\bar{C}$ are both maximized at the same AV level set $\{N_a^j, \forall j \in J\}$. Thus, we maximize the adjusted capacity. The first order condition for maximizing $\bar{C}$ w.r.t. any N_a^j gives

$$\frac{\sum_j p^j N_r^j (\beta_a^1/\beta_r^j)^\gamma (1 + l)}{\sum_j p^j N_r^j (\beta_a^1/\beta_r^j)^\gamma (1 + l) + \sum_j p^j N_r^j (\beta_a^1/\beta_r^j)^\gamma} = 1 - \frac{c_a}{2(c_a - c_r)} + \frac{1}{2\tau(1 + l) - 2} \tag{63}$$

where $\tau = (\beta_r^j/\beta_a^j)^{1/\gamma}, \forall j \in J$. The LHS of (63) is equivalent to the automation ratio $r = v_a/v$ if we multiply the numerator and denominator by x_a^1. Thus, to maximize the adjusted capacity, we need to keep the automation ratio at its optimal value r^*, which is the RHS of (63). We find (28a) and (28c) by setting the RHS of (63) equal to 1 and 0, respectively.

Appendix B: Heterogeneous households

In this appendix, we present results from the simulation model with heterogeneous time costs. Similar to Section 6 we assume a regular household time cost of $\beta_r = 14$. For AV households, we

randomly generate the time cost of each OD pair (i, j) from the truncated Normal distribution with a mean of $\bar{\beta}_a^{ij} \in \{14, 17.5, 20\}$ and a variance of $\sigma^2 = 1$ bounded from below by $\beta_r = 14$. We present the social welfare of the heterogeneous and homogeneous time costs in Fig. 9. We observe that the two social welfare curves follow the same trend and the optimal levels of automation are close.

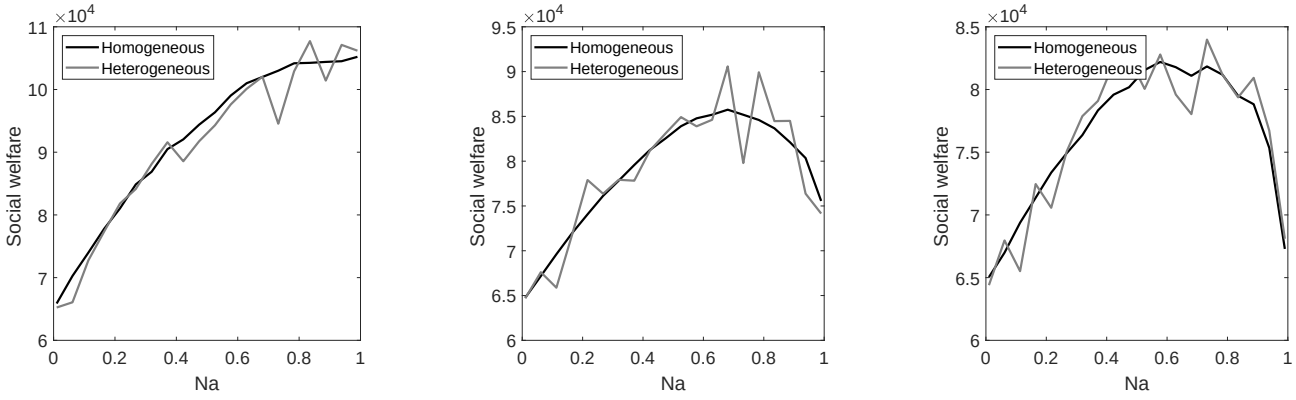

Figure 9: Simulation results at heterogeneous and homogeneous time costs. Parameters are from the GTAModel V4.0 (2019) and the Transportation Tomorrow Survey (2019). The expected AV time costs are a) $\bar{\beta}_a^{ij} = 20$, b) $\bar{\beta}_a^{ij} = 17.5$, and c) $\bar{\beta}_a^{ij} = 14$.

Appendix C: Peer to peer sharing

In this Appendix we present an analytical model to derive the fleet size of the peer to peer sharing business model. Consider the peer to peer sharing model where n households share m AVs and each AV household pays $f_a = mF_a/n$. To account for these trips, we assume that the relocation load in the network is a function $l = L(m, n)$ per trip.

Each vehicle may be in one of three states: (i) en route to the destination of the passengers on board, (ii) driving to pick up passengers from their origin location, and (iii) waiting (idle) to be requested by passengers. According to Little's law (Little, 2011), under steady state conditions, there are nx_aT AVs that are en route to a destination, because the trip generation rate of the coalition is nx_a and the duration of each trip is T. Under the same steady state conditions, there are nx_alT vehicles dispatched to pick up passengers, where lT is the expected driving time of zombie trips. Note that because $l \leq 1$, then $lT \leq T$; i.e., the relocation trips are shorter than regular trips with passengers on board.

We assume that users are willing to wait lT. As this wait time threshold decreases, we need more AVs in idle state waiting for the next request. Daganzo (2010) develops a similar sharing model (for taxis) where idle vehicles are uniformly distributed over a region, and shows that the required number of idle vehicles is $A/(lT)^2$ where A is a parameter related to the size of the service

region. Combining the threshold, lT, with the results in Daganzo (2010) [Chapter 5, page 5-4] we get the required fleet size, m, as:

$$m = nx_aT + nx_alT + \frac{A}{(lT)^2}. \tag{64}$$

The fleet size, m, affects the vehicle sharing cost, $f_a = mF_a/n$, and consequently the net utility of AV households. We note that (64) does not capture the pooling effect (i.e., the possibility of fewer relocation trips due to the network properties) in AV sharing.

We individually investigate the three Cases of Fig. 2. In Cases I and III, the AV household trips x_a^* and the travel time T are independent of the sharing contract (m, n) because there is an all-or-nothing user equilibrium solution: when $N_a^\circ = 1$ (in Case I), there exists a unique x_a^* (and T) that are used in (64) to find the fleet size m. In contrast, if $N_a^\circ = 0$, then there are no AV households and the sharing arrangement is irrelevant.

Case II is not as straightforward, because the user equilibrium solution may be an intermediate point $N_a^\circ \in (0, 1)$ as shown in Fig. 5c and 5g. For a given contract (m, n), we find x_a^* (and N_a°) that may require an updated fleet size per (64). For a given m, we find x_a^* (using the equilibrium conditions), and then use x_a^* to find a new m using (64). We iterate between updating m and x_a^* until convergence.

In Fig. 10a, we present the RHS of (64) for different number of household trips x_a and coalition size n. We bound the fleet size m by the coalition size n, otherwise it would be more beneficial if each household owns a personal AV instead of sharing. Fig. 10a illustrates an EOQ-shape of (64). In Fig. 10b, we present the contract structure (m, n) at different l derived from the iterative process above. Therefore, the acceptable relocation load l increases, the fleet size m and the coalition size n both decrease.

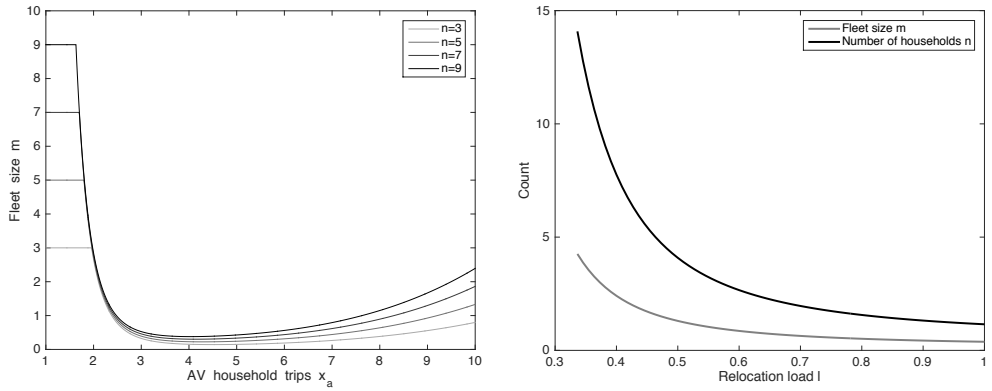

Figure 10: (a) Fleet size as function of x_a and n per (64); (b) Fleet and coalition size as a function of the acceptable relocation load l. Count refers to the number of AVs and the number of households.